

Northumbria Research Link

Citation: Ng, Zhi Lin, Hernández-Molina, F. Javier, Duarte, Débora, Sierro, Francisco J., Ledesma, Santiago, Rogerson, Michael, Llave, Estefanía, Roque, Cristina and Manar, M. Amine (2021) Latest Miocene restriction of the Mediterranean Outflow Water: a perspective from the Gulf of Cádiz. *Geo-Marine Letters*, 41 (2). p. 23. ISSN 0276-0460

Published by: Springer

URL: <https://doi.org/10.1007/s00367-021-00693-9> <<https://doi.org/10.1007/s00367-021-00693-9>>

This version was downloaded from Northumbria Research Link:
<http://nrl.northumbria.ac.uk/id/eprint/46194/>

Northumbria University has developed Northumbria Research Link (NRL) to enable users to access the University's research output. Copyright © and moral rights for items on NRL are retained by the individual author(s) and/or other copyright owners. Single copies of full items can be reproduced, displayed or performed, and given to third parties in any format or medium for personal research or study, educational, or not-for-profit purposes without prior permission or charge, provided the authors, title and full bibliographic details are given, as well as a hyperlink and/or URL to the original metadata page. The content must not be changed in any way. Full items must not be sold commercially in any format or medium without formal permission of the copyright holder. The full policy is available online: <http://nrl.northumbria.ac.uk/policies.html>

This document may differ from the final, published version of the research and has been made available online in accordance with publisher policies. To read and/or cite from the published version of the research, please visit the publisher's website (a subscription may be required.)

1 **Latest Miocene restriction of the Mediterranean Outflow Water: A perspective from the Gulf of**
2 **Cádiz**

3 Zhi Lin Ng^{1*}, F. Javier Hernández-Molina¹, Débora Duarte^{1, 2}, Francisco J. Sierro³, Santiago Ledesma⁴, Michael
4 Rogerson⁵, Estefanía Llave⁶, Cristina Roque^{7, 8}, M. Amine Manar⁹

5 ¹Dept. Earth Sciences, Royal Holloway Univ. London, Egham TW20 0EX, UK

6 ²Instituto Português do Mar e da Atmosfera (IPMA), 1749-077 Lisboa, Portugal

7 ³Dpto. de Geología, Univ. de Salamanca, 37008 Salamanca, Spain

8 ⁴Naturgy Energy Group S.A., 28033 Madrid, Spain

9 ⁵Dept. Geography and Environmental Sciences, Northumbria Univ., Newcastle upon Tyne, NE1 8ST, UK

10 ⁶Instituto Geológico y Minero de España (IGME), 28003 Madrid, Spain

11 ⁷Estrutura de Missão para a Extensão da Plataforma Continental (EMEPC), 2770-047 Paço de Arcos, Portugal

12 ⁸Instituto Dom Luiz (IDL), 1749-016 Lisboa, Portugal

13 ⁹Office National des Hydrocarbures et des Mines (ONHYM), BP 99 Rabat, Morocco

14 Corresponding author: Zhi Lin Ng (Zhi.Ng.2016@live.rhul.ac.uk)

15 **Abstract**

16 The Mediterranean-Atlantic water-mass exchange provides the ideal setting for deciphering the role of gateway
17 evolution in ocean circulation. However, the dynamics of Mediterranean Outflow Water (MOW) during closure of
18 the Late Miocene Mediterranean-Atlantic gateways are poorly understood. Here, we define the sedimentary evolution
19 of Neogene basins from the Gulf of Cádiz to the West Iberian margin to investigate MOW circulation during the latest
20 Miocene. Seismic interpretation highlights a middle to upper Messinian seismic unit of transparent facies, whose base
21 predates the onset of the Messinian Salinity Crisis (MSC). Its facies and distribution imply a predominantly
22 hemipelagic environment along the Atlantic margins, suggesting an absence or intermittence of MOW preceding
23 evaporite precipitation in the Mediterranean, simultaneous to progressive gateway restriction. The removal of MOW
24 from the Mediterranean-Atlantic water-mass exchange reorganised the Atlantic water-masses and is correlated to
25 severe weakening of the Atlantic Meridional Overturning Circulation (AMOC) and a period of further cooling in the
26 North Atlantic during the latest Miocene.

27 **Introduction**

28 Gateway evolution plays a significant role in the reorganisation of global ocean circulation (Berggren, 1982;
29 Knutz, 2008; Straume et al. 2020). The Mediterranean-Atlantic water-mass exchange provides the ideal setting for
30 such research. At present, the Mediterranean-Atlantic exchange is characterized by an anti-estuarine circulation (Wüst,
31 1961) involving a surficial Atlantic inflow and a deeper outflow, known as the Mediterranean Outflow Water (MOW),

32 through the Strait of Gibraltar (Sánchez-Leal et al., 2017). The MOW is predominantly sourced from the intermediate
33 water-mass of the Mediterranean, known as the Levantine Intermediate Water (LIW) (Millot et al., 2006). Upon
34 exiting the Strait of Gibraltar, the dense MOW cascades onto the Gulf of Cádiz continental slope, entraining or mixing
35 with Atlantic ambient water to form the Atlantic Mediterranean Water (AMW) (Rogerson et al., 2012b). The entrained
36 ambient water is mainly sourced from the Azores Current, which originates at the Azores Front, the boundary between
37 the European and African surface water-masses (Rogerson et al., 2004). The resulting AMW water-mass settles along
38 the middle continental slope (~1000–1500 m) and flows northwards above the North Atlantic Deep Water (NADW)
39 (O'Neill-Baringer and Price, 1997; Hernandez-Molina et al., 2016). MOW input into the Atlantic has a significant
40 impact on the formation of the NADW and on the thermohaline circulation (Pérez-Asensio et al., 2012), known as the
41 Atlantic Meridional Overturning Circulation (AMOC). Removal or interruption of MOW would significantly impact
42 the AMOC by ~15% and reduce sea surface temperatures by up to 1°C (Rogerson et al., 2012b). The AMOC plays a
43 vital role in the earth's climate through the northward transport of heat and CO₂, which bears an impact on the Arctic
44 sea ice volume (Liu et al., 2020) and the ocean-terrestrial carbon cycle (Zickfeld et al., 2008).

45 The Mediterranean-Atlantic exchange was also active through the Late Miocene gateways (Fig. 1; ~11.6 –
46 6.9 Ma; Krijgsman et al., 2018), which include the Betic and Rifian corridors currently exposed onshore southern
47 Spain and northern Morocco, respectively (Capella et al., 2017), and possibly the Strait of Gibraltar (Krijgsman et al.,
48 2018). It is thought to have ceased or become reduced during the latest Miocene, causing isolation of the
49 Mediterranean Sea from the Atlantic Ocean, hence the Messinian Salinity Crisis (MSC; 5.97–5.33 Ma; Krijgsman et
50 al., 1999; Manzi et al., 2018). However, since formulating the MSC concept, Selli (1960) also argued for the early
51 Messinian (~7.25 Ma) as the actual beginning of the MSC; it is marked by dystrophic faunal elements in the
52 Mediterranean as the earliest indication of an ongoing restriction of the exchange. Yet restriction of MOW from the
53 Mediterranean-Atlantic water-mass exchange is one of the prerequisites for hypersaline conditions to deposit MSC
54 evaporites (Flecker et al., 2015). In the Mediterranean, an inferred base-level fall and erosion of its margins during
55 the MSC acme, and subsequent refilling by an open marine connection with the Atlantic, respectively resulted in a
56 regional Messinian erosional surface (MES; 5.61 Ma), and a sharp lithological and paleontological change across the
57 Miocene-Pliocene boundary (5.33 Ma) (Roveri et al., 2014). In turn, the onset of the MSC (5.97 Ma) shows no
58 correlation to glacio-eustatic change, and was thought to be controlled dominantly by tectonics (Flecker and Ellam,
59 2006; Hodell et al., 2001; Krijgsman et al., 2004).

60 In the Atlantic domain, open marine conditions have prevailed throughout the Miocene to the present (Flecker
61 et al., 2015). Locally, the continental margins surrounding the Gulf of Cádiz were affected by gravitational processes
62 due to rapid regional uplift and tectonic instability after the Middle to Late Miocene Betic-Rif Orogeny (Duggen et
63 al., 2003). The Betic-Rif Orogeny, due to convergence between Africa and Eurasia, transformed a wider Middle
64 Miocene gateway (~15 Ma) into several Late Miocene narrow and shallow corridors (~8 Ma) affecting MOW
65 distribution, namely: the North Betic Strait, Guadix Basin, Zagra Strait, Guadalhorce Strait, and the North and South
66 Riffian Corridors. (Fig. 1; Capella et al., 2019; Krijgsman et al., 2018). The continuous constriction and closure of
67 these corridors and the reduction of the water-mass exchange are collectively known as the Mediterranean-Atlantic
68 gateway restriction (Krijgsman et al., 2018; Pérez-Asensio et al., 2012). The distribution of contourite depositional
69 systems within these corridors serves as evidence of bottom current influence from the MOW as it exits the
70 Mediterranean (de Weger et al., 2020; Martín et al., 2009). The increase in bottom-current velocities as a consequence
71 of the ongoing restriction of the corridors, and the initiation of an overflow setting for the MOW across the
72 Mediterranean-Atlantic water-mass exchange, resulted in the deposition of sandy contourites in the Betic and Riffian
73 Corridors during the late Tortonian to early Messinian (7.8 – 7.25 Ma; Capella et al., 2017; de Weger et al., 2020;
74 Martín et al., 2009), but has yet to be described for the Gulf of Cádiz. During this period, the Gulf of Cádiz would
75 have represented the downstream continuation of the Betic and Riffian Corridors for MOW circulation after exiting
76 the Mediterranean. Relocation of the contourite depositional system to the Gulf of Cádiz, within the Deep Algarve,
77 Doñana, Sanlúcar and Cádiz basins (Fig. 1), occurred from Pliocene to the present (5.33 Ma onwards), with the MOW
78 flowing through the Strait of Gibraltar (Hernández-Molina et al., 2014; 2016). However, the Strait of Gibraltar might
79 have opened earlier in the early Messinian (Krijgsman et al., 2018). Meanwhile, the Guadalquivir and Onshore Gharb
80 basins (Fig. 1), located at the western end of the Betic and Riffian corridors, became marine embayments after the
81 closure of these corridors (Capella et al., 2017; Pérez-Asensio et al., 2012). Despite extensive outcrop studies carried
82 out onshore, the timing of final closure of the gateways remains unknown, due to erosional hiatuses in the sedimentary
83 record (Capella et al., 2017; Hüsing et al., 2010). Some outcrop studies suggest that the closure of the gateways
84 occurred well before the onset of the MSC (Kouwenhoven et al., 1999; Martin et al., 2002), whereas modeling studies
85 suggest that a narrow (~1 km) and shallow (~10m) connection is sufficient to supply the salt for the MSC evaporites
86 (Meijer and Krijgsman, 2005).

87 Here, we define the middle to late Messinian sedimentary evolution and its relationship with its upper and
88 lower bounding stratigraphic units in the Neogene basins (Offshore Gharb, Deep Algarve, Doñana, Sanlúcar, Cádiz
89 and Alentejo basins), located on the upper to middle continental slope of the Northwest Moroccan (NWMM), the
90 Southwest Iberian (SWIM), and the southern part of the West Iberian (WIM) margins (Fig. 1) using seismic
91 stratigraphic analysis, correlated to chronology and lithology from borehole data (Fig. 2). We compared the
92 distribution of the middle to upper Messinian succession with the Guadalquivir and Onshore Gharb basins (Fig. 1),
93 based on the literature, to evaluate its significance for the Mediterranean-Atlantic water-mass exchange and its
94 implications for sedimentary and paleoceanographic processes in the Atlantic. For the first time, we investigated the
95 paleoceanographic scenarios for the Late Miocene Mediterranean-Atlantic water-mass exchange through a
96 hypothetico-deductive method, using a simple quantitative representation of the system together with seismo-
97 stratigraphic evidence and observations.

98 **Materials and Methods**

99 Seismic analysis and borehole correlation

100 We compiled a regional database of seismic reflection and borehole data in the Gulf of Cádiz to the southern
101 part of the West Iberian Margin (Fig. 1). We carried out seismic interpretation of the database, which entailed the
102 identification of seismic facies and boundaries, focusing on the middle to late Messinian unit. We utilized the
103 nomenclature for seismic facies description and interpretation of Prather et al. (1998) based analogously on an
104 intraslope basin setting in the Gulf of Mexico, which characterized three primary seismic facies categories (chaotic,
105 convergent and draping). The seismic stratigraphy were correlated to borehole data (Fig. 2) consisting of lithological
106 and chronological information (Table S1). They include five wells available from the literature: Algarve-2
107 (Hernández-Molina et al., 2016), Atlantida-3 and Golfo de Cádiz B-3 (GCB-3; Ledesma, 2000), Golfo de Cádiz Mar
108 Profundo C-1 (GCMPC-1; Hernández-Molina et al., 2014), and U1387 (van der Schee et al., 2016); three additional
109 wells: Anchois-1, Deep Thon-1, and Merou-1, were acquired from an internal report for petroleum exploration by
110 Repsol S.A., titled “*Tanger-Larache Sedimentological study*” (hereinafter referred to as Repsol S.A., 2013). The
111 chronological information is based on bio- and cyclo-stratigraphic dating acquired from boreholes with top-only
112 penetration of the middle to late Messinian unit in U1387 (van der Schee et al., 2016) and Algarve-2 (Hernández-

113 Molina et al., 2016), while its base is reached in Atlantida-3 and GCB- 3 (Ledesma, 2000), GCMPC-1 (Hernández-
114 Molina et al., 2014), Anchois-1, Deep Thon-1 and Merou-1 (Repsol S.A., 2013) (Table S1).

115 Quantitative exploration of past flow conditions

116 We adopted simple quantitative representations below to test three possible scenarios through a hypothetico-
117 deductive method, based on the climatic, paleogeographic and paleoceanographic conditions during the middle to late
118 Messinian, where a two-way water-mass exchange between the Atlantic and the Mediterranean could be active. These
119 experiments directly test hypotheses drawn from seismic and borehole analysis, which is limited to determining the
120 presence or absence of flow on the slope, and the bottom velocity thresholds required for muddy and sandy bedform
121 deposition. Key to the latter is the threshold at which sandy contourite deposition commences, as we expect deposits
122 of this nature to be resolved in seismic data as packages with variable impedance. Field and experimental works (eg.
123 Culp et al., 2020; McCave et al., 2017; McCave and Hall, 2006) indicate that winnowing of muddy marine sediments
124 and construction of muddy bedforms occur at flow velocities higher than 0.15 m s^{-1} , while winnowing, reworking and
125 accumulation of sandy marine sediments occur at flow velocities higher than 0.2 m s^{-1} . Consequently, the maximum
126 MOW or AMW plume velocity on the Gulf of Cádiz upper to middle slope for the middle to late Messinian, where
127 no contourite deposition is observed within the seismic resolution of our dataset, would be 0.2 m s^{-1} , while the physical
128 oceanography of the exchange must be consistent with generating flow no faster than this value. We also investigated
129 a MOW or AMW plume velocity of 0.15 m s^{-1} for the threshold of silt-rich muddy contourite formation by bottom
130 currents. Three scenarios allowing for a continuing MOW are explored here:

- 131 • Scenario A: The flux of exchange (and thus the size of the plume) were so small that the area impacted on
132 the slope could not be resolved by the seismic analysis;
- 133 • Scenario B: The flow was slower during the middle to late Messinian than it was during the late Tortonian
134 to early Messinian, where contourite deposition can be observed; and
- 135 • Scenario C: The seismic analysis does not cover the region over which the MOW or AMW was flowing
136 during the middle to late Messinian.

137 Following previous intensive research into these relationships (Rogerson et al., 2012a; Simon and Meijer, 2015), we
138 used *equations 1 – 6* to represent the system,

$$\frac{Q_{MOW}}{Q_{Inflow}} = 1 / \left(\frac{S_M}{S_A} \right) \quad (1) Q_{AMW} = Q_{MOW} / \Phi$$

$$\Phi = 1 - \frac{B_{geo}^{1/3}}{U_{geo}} \quad (3)$$

$$B_{geo} = \frac{H_{MOW} U_{MOW} g'}{(1 + 2K_{geo} x / w_{MOW})} \quad (4)$$

$$U_{geo} = g' \alpha / f \quad (5)$$

$$g' = \frac{\rho_{AMW} - \rho_{ATL}}{\rho_{AMW}} \quad (6)$$

145 where Q_{inflow} , Q_{AMW} and Q_{MOW} (Sv) are respectively the fluxes of Atlantic inflow, AMW, and MOW; S_M and S_A
 146 (PSU) are the salinities of the Mediterranean and Atlantic water, respectively; Φ is the mixing coefficient of AMW
 147 and MOW; B_{geo} and U_{geo} ($m s^{-1}$) are geostrophic buoyancy flux and velocity, where B_{geo} is measured by H_{MOW} (m),
 148 U_{MOW} ($m s^{-1}$) and w_{MOW} (m), which are the height, velocity and width of pure MOW at the gateway, K_{geo} ($m s^{-1}$), which
 149 is the geostrophic Ekman number (assumed 0.2), and x (m), which is the distance downslope from which mixing or
 150 entrainment occurs (assumed 100,000 m,; while U_{geo} is measured by g'_{\perp} , which is the density anomaly of the plume
 151 within the ambient water, α , which is the slope the water is moving over, and f , which is the acceleration due to
 152 Coriolis force (assumed $0.000084 m s^{-2}$); g' is determined from ρ_{AMW} and ρ_{ATL} ($kg m^{-3}$), which are respectively the
 153 densities of AMW and ambient Atlantic water (Rogerson et al., 2012b).

154 Today, the velocity of water (U_{geo}) interacting with bedform-dominated sediment surfaces varies between 1.4
 155 $m s^{-1}$ for regions with sandy contourites or abrasion surfaces to 0.3-0.5 $m s^{-1}$ for muddy contourites (O'Neill-Baringer
 156 and Price, 1999). The higher velocities in proximal parts of the system reflect the presence of an unmixed core of
 157 MOW water which is yet to frictionally entrain ambient Atlantic water, and thus relates directly to the modern salinity
 158 difference of Mediterranean and Atlantic water of ~ 2 PSU (Rogerson et al., 2012b). The lower velocities in the distal
 159 part of the system reflect water almost completely mixed to produce AMW (Atlantic Mediterranean Water)
 160 composition, and thus relates to the density of the plume of water that lies at neutral density in the Atlantic.

161 **Results**

162 Seismic Analysis

163 Seismic interpretation of the Gulf of Cádiz continental slope shows three main sedimentary intervals above a basin-
164 wide erosional unconformity known as the Basal Foredeep unconformity (BFU; ~8.2 Ma, sensu Maldonado et al.,
165 1999). The BFU is juxtaposed against a thick chaotic body pinching out northwards, known as the Allochthonous Unit
166 of the Gulf of Cádiz (AUGC; Fig. 2; sensu Medialdea et al., 2004). Above the BFU, an upper Tortonian-lower
167 Messinian (~8.2 – ~6.4 Ma) succession consisting of high-amplitude convergent-by-basalap facies (Fig. 3b) is
168 observed along the Southwest Iberian margin. In the Northwest Moroccan margin and the southern part of the West
169 Iberian margin, the upper-Tortonian-lower Messinian succession consists of cyclical alternations of low-to-high-
170 amplitude reflections in sheeted or mounded geometries adjacent to basin margins (Fig. 3, a and c). The top of the
171 upper Tortonian-lower Messinian succession is bounded by, or locally truncated against, an unconformity.

172 Overlying the upper Tortonian-lower Messinian succession is a middle-upper Messinian seismic unit of
173 transparent seismic facies or with seismic reflections of very low amplitude, locally underlain by high-amplitude
174 reflections (Fig. 2 and 3). It has a relatively homogenous reflection configuration, in sheeted or draped geometries.
175 The base is erosional at basin margins with locally high-amplitude chaotic facies (Fig. 3b) with a “gull-wing” geometry
176 (*sensu* Wynn et al., 2007) and onlap to downlap terminations (Fig. 3c). The basal boundary could also be conformable
177 on older successions in the basin centers (Fig. 2b). Within the Offshore Gharb basin, the transparent reflections are
178 interrupted by intervals of high amplitude convergent-by-thinning facies in the basin centre and high amplitude chaotic
179 facies at the basin margin (Fig. 2b and 3c), whereas away from the basin this unit can be observed as draping facies
180 at the margins (Fig. 3c). Across the upper to middle slope of the Gulf of Cádiz, the tabular distribution of the middle
181 to upper Messinian unit is also punctuated by structural highs (Fig. 2a) and areas of erosion (Fig. 4), or depocenters
182 with the presence of high amplitude chaotic or convergent facies, most prominently the eastern section of the Deep
183 Algarve basin and the Offshore Gharb basin (Fig. 2b and 3a).

184 The top boundary of the middle-upper Messinian seismic unit is generally conformable with a change from
185 transparent to a relatively continuous seismic facies (Fig. 2b and 3b), or locally unconformable as truncation surfaces
186 against younger successions (Fig. 3a), represented by the Miocene-Pliocene boundary (MPB; 5.33 Ma; *sensu*

187 Hernandez-Molina et al., 2016). The Pliocene-Quaternary (5.33 Ma – present) succession above consists of lowermost
188 Pliocene low- to moderate-amplitude parallel continuous facies in the basin centres, or lower Pliocene high-amplitude
189 chaotic facies on the basin margins truncating the lowermost Pliocene units. They are overlain by upper Pliocene-
190 Quaternary cyclical alternation of low- to high- amplitude sequences in sheeted to mounded geometries associated
191 with alongslope channels (Fig. 3, a and c), or prograding clinoforms in the north- and southeast originating from lower
192 Guadalquivir and Onshore Gharb basins, respectively (Fig. 3b).

193 The contrast in seismic facies between the middle-upper Messinian unit with the upper Tortonian-lower
194 Messinian and Pliocene-Quaternary succession below and above, respectively, provides a distinctive signature for
195 regional stratigraphic correlation across the Gulf of Cádiz towards the southern part of the West Iberian margin (Fig.
196 2 and 3) and can be considered as a regional marker horizon or stratigraphic unit. The middle to upper Messinian unit
197 has an average thickness of 100 ms TWT (with a range of 50-150 ms TWT), distributed uniformly across the upper
198 to middle continental slope, as shown by the time thickness map of the middle to late Messinian unit (Fig. 4). An
199 exception is observed for the Offshore Gharb basin in the Northwest Moroccan margin, with distribution of the middle
200 to upper Messinian unit reaching up to 1200 ms TWT in thickness (Fig. 2b and 4). Likewise, a thicker distribution for
201 the upper Tortonian-lower Messinian succession is observed for the Northwest Moroccan margin and the southern
202 part of the West Iberian margin (500-1000 ms TWT), in contrast to the Southwest Iberian Margin (250-500 ms TWT).

203 Borehole Correlation

204 Correlation of the middle to upper Messinian unit to borehole data indicates fossiliferous marls to clays with
205 distinct bioturbation, containing few lithic coarser particles (Hernandez-Molina et al., 2014; van der Schee et al.,
206 2016), with a mean interval velocity (V_{int}) of $\sim 2290\text{--}2570\text{ m s}^{-1}$ based on check-shot data from Algarve-2 and
207 GCMPC-1. In the Offshore Gharb basin, this interval is recorded in Anchois-1, Deep Thon-1 and Merou-1 as very
208 shaly or dirty unconsolidated sands with intercalations of clays (Repsol S.A., 2013). Bio- and cyclo-stratigraphic
209 dating (Fig. 2 and 5; Table S1) show deposition of the unit spanning an interval of $\sim 1.1\text{ Ma}$ ($>6.37\text{--}5.33\text{ Ma}$), with
210 the base predating the First Occurrence (FO) *Globorotalia margaritae*, Last Regular Occurrence (LaO) or Last
211 abundant Occurrence (LaO) *Globorotalia miotumida* events dated 6.31 to 6.35 Ma, and the sinistral to dextral coiling
212 change of the *Neogloboquadrina acostaensis* event dated 6.37 Ma (Krijgsman et al., 2004).

213 Quantitative Constraint on Changes in the Oceanographic System

214 Assuming an absence of contourite deposition within the seismic resolution of our dataset, the critical
215 requirement for a continuing MOW in the Gulf of Cádiz is the flow velocity threshold of 0.2 m s⁻¹ for the onset of
216 winnowing and accumulation of sands (McCave and Hall, 2006). Additionally, the 0.15 m s⁻¹ threshold where
217 winnowing and silty bedform construction begins (Culp et al., 2020; McCave et al., 2017) is considered. Three
218 scenarios would permit MOW to continue across the Mediterranean-Atlantic water-mass exchange but be invisible
219 under the resolution of our seismic analysis: A) a very small plume (due to considerably reduced flux), B) a plume
220 flowing very slowly, and C) the plume has moved out of the analyzed area. All three possibilities are
221 investigated. Unless one of these scenarios is capable of producing the sedimentary features observed above, the
222 exchange must have been different from that found today.

223 Two critical constraints on the system are revealed by *equations 1-6* (presented in *Material and Methods*), which
224 reflect two inverse relationships: firstly between flux and salinity, and secondly between salinity and ambient water
225 entrainment. During the salinification of the Mediterranean, small fluxes of the Mediterranean-Atlantic water-mass
226 exchange at the sill correlate to high salinity in the outflowing Mediterranean water (via *equation 1*). This relationship
227 is explored in detail in Simon and Meijer (2015), and we adopt their conclusions here. Accordingly, a high salinity or
228 density in the outflowing Mediterranean water would result in a high velocity MOW (via *equations 5 and 6*), an
229 intense frictional mixing with ambient water as it passes over the sill of the Mediterranean-Atlantic gateways (via
230 *equation 3*) and hence a vigorous formation of AMW (Rogerson et al., 2012b). Consequently, as the flux of MOW
231 (Q_{MOW}) falls, its mixing or entrainment behaviour (Φ) also changes (via *equation 2*). Where Q_{MOW} is below modern
232 values (~0.68 Sv), these influences balance, providing the counter-intuitive result that the flux of AMW (Q_{AMW}) is
233 almost invariable. The behaviour is best illustrated via the relationship between Φ (Phi) and velocity (see Fig. S1 in
234 *supplementary material*). Consequently, a very small flux of very saline water would, under a first approximation,
235 generate a geostrophic current similar to today, and hence a contourite depositional system in the Gulf of Cádiz.

236 This inverse and non-linear relationship between MOW salinity and entrainment of ambient Atlantic water
237 complicates the relationship of the Mediterranean-Atlantic water-mass exchange at the sill, and the expected response
238 in both the Gulf of Cadiz and the Mediterranean to changes in other oceanographic conditions. Under freshening
239 scenarios, a reduced salinity or density, and hence velocity (via *equations 5 and 6*), for the MOW flowing into the

240 Atlantic would suppress entrainment (via *equation 3*), resulting in an almost unchanged AMW compared to pure
241 MOW post-mixing. This control essentially acts as a negative feedback to changes in the system, which maintains the
242 physical size of the flux. Consequently, a slower outflow would reflect a less-dense water-mass in the Mediterranean.
243 Overall, the resulting dynamics between the physical properties of the Mediterranean-Atlantic water-mass exchange
244 described above are significant for constraining scenarios to discuss the possibility of a continuing outflow across
245 the Mediterranean-Atlantic gateways, complementary to our observations in the seismic and sedimentary
246 interpretation presented in this study.

247

248 **Discussion**

249 Stratigraphic and Sedimentary Interpretation

250 The middle to upper Messinian unit (~6.4 – 5.33 Ma) is equivalent to the previously described lower section
251 of Marismas Sequence in Riaza and Martínez del Olmo (1996), Unit M3 in Maldonado et al. (1999), Unit MW3' in
252 Roque (2007), Subunit U1B in Rodrigues (2017), and Subunit E2 in Lopes et al. (2006). Similar successions are found
253 in the subsurface of the onshore Guadalquivir basin as Gibraleón clays (Sierro et al., 1996) or Unit C in Ledesma
254 (2000), and in the Onshore Gharb basin (Capella et al., 2017) when they were marine embayments following gateway
255 closures (Martín et al., 2009; Ivanovic et al., 2013). These previous works interpreted similar seismic and sedimentary
256 characteristics for the middle to upper Messinian unit (eg. transparent zones and thick clay deposits) and confirm its
257 stratigraphic position in the margin.

258 The seismic and sedimentary facies, and the widespread uniform and tabular distribution of the middle to
259 upper Messinian unit across the continental margins (Fig. 2 and 3), imply dominant deposition of hemipelagic settling
260 in the absence of alongslope transport. A higher estimated rate of accumulation (5.2-17.5 cm ka⁻¹) compared to the
261 average hemipelagic sedimentation rate (2 cm ka⁻¹, McCave and Hall, 2006) could be due to higher influx of
262 allochthonous terrigenous material on the continental slopes (Henrich and Hüneke, 2011). Higher sedimentation rates
263 within the intraslope basins, such as the eastern Deep Algarve (Fig. 3b) and Offshore Gharb (Fig. 2b and 3c) basins,
264 are due to interruption in the background sedimentation by interbedded deposition of deep-water turbidite channel-
265 levees and lobes or debrites by gravity flow originating from the adjacent margins, or from the Guadalquivir and

266 Onshore Gharb basins, respectively (Ledesma, 2000). This is indicated by the interpretation of adjoining development
267 of local intervals of high-amplitude chaotic to channel facies on the basin margin and high-amplitude convergent
268 facies locally within the basin centres, as opposed to the transparent draping facies observed regionally across the
269 margin. In the Offshore Gharb basin, the middle-upper Messinian unit consists of a distal turbidite depositional
270 environment of deep-water channels or lobes interbedded with hemipelagic drapes, as interpreted in the Anchois-1,
271 Deep Thon-1 and Merou-1 wells (Repsol S.A., 2013).

272 Underlying the middle to upper Messinian unit, contourite deposits are distributed onshore and offshore
273 Morocco (Capella et al., 2017; de Weger et al., 2020) as well as in the southern part of the West Iberian margin
274 (Rodrigues, 2017) due to the MOW. This indicates an active exchange through the Riffian Corridor until early
275 Messinian, whereas synchronous MOW influence in the Deep Algarve and Guadalquivir basins has not been reported
276 to date. The fact that the upper Tortonian-lower Messinian sequence in the Northwest Moroccan margin is thicker
277 than in the Southwest Iberian margin could also reflect higher sedimentary input with an active MOW through a
278 connected Riffian but a dormant Betic corridor. However, because of the absence of field evidence onshore Morocco
279 for a marine connection above Lower Messinian deposits (Capella et al., 2019), a shift in MOW circulation through
280 the Strait of Gibraltar cannot be excluded (Krijgsman et al., 2018) with currently available drilling information.

281 Meanwhile, the top of the middle to upper Messinian unit relates to the end of the MSC, marking a lithological
282 shift from middle to late Messinian hemipelagic conditions into lowermost Pliocene contourite deposits formed by the
283 initiation of weak MOW through the Strait of Gibraltar from 5.33 to 3.2 Ma (Hernández-Molina et al., 2016), with the
284 presence of contourite bigradational sequences directly above the Miocene-Pliocene boundary and an abrupt change
285 in sedimentation rate from 10 to 27 cm ka⁻¹ (van der Schee et al., 2016). This change is in agreement with the
286 instantaneous return to open marine connection observed in the Mediterranean (Roveri et al., 2014). The middle to
287 late Messinian and lowermost Pliocene sediments could also be truncated by younger lower Pliocene gravity flow
288 deposits, either channel-filled turbidites, debrites, or slope fans originating from the margins (~5.2–3.8 Ma) (Ducassou
289 et al., 2016; Sierro et al., 2008). They are caused by compressional tectonics superimposed upon glacio-eustatic
290 variation (Pérez-Asensio et al., 2018; Sierro et al., 2008).

291 Quantitative Testing of Paleoceanographic Conditions through Hypothetico-Deductive Method

292 The finding that contourite deposition is not evidenced within the Gulf of Cádiz at seismic scale during the
293 deposition of the middle to upper Messinian unit can be interpreted in several ways. It is even possible that MOW
294 flow did continue, despite not being resolved in our body of data. Here, the viability of continuing but changed
295 alongslope flow is explored quantitatively using the simple representation of the plume outlined in *Materials and*
296 *Methods*, and the physical constraints on the behaviour of the system described in *Results*. Below we discuss the three
297 scenarios put forth in *Results*, and possible no-analog exchanges as an explanation for our observations at the end of
298 this section.

299 *Could there be a very small flux?*

300 Given the necessity for the conservation of salt and mass in marginal basin exchanges like the Mediterranean-
301 Atlantic connection at the Strait of Gibraltar, a reduced flow of water must result in greater density (Bryden et al.,
302 1993). The absolute magnitude of the fluxes would then reflect the underlying control from the net freshwater export
303 flux for the Mediterranean basin, which is 0.05 Sv (Bethoux and Gentili, 1999). This control has been modelled for
304 the Messinian context (Simon and Meijer, 2015), and a small flux exchange is highly consistent with the evolution of
305 a more saline Mediterranean water-mass. Under halite-depositing conditions (Roveri et al., 2014), the flux could be
306 orders of magnitude less than today. As described in *Results*, the small flux would lead to a high density and velocity
307 MOW with more intense mixing, and the subsequent vigorous formation of AMW, generating a geostrophic current
308 capable of forming a contourite depositional system in the Gulf of Cádiz similar to that observed during the Pliocene
309 and Quaternary (Hernández-Molina et al., 2014; 2016). Thus, while superficially attractive, it is not likely that the
310 absence of contourite deposits in the cores and seismic presented in this study can be explained by a very small flux
311 at the gateway.

312 *Could there be a slower flow?*

313 In terms of the paleo-AMW plume, the maximum flow velocity in the region during the middle to late Messinian
314 consistent with our observations (absence of contourite depositional system) is 0.2 m s^{-1} (McCave and Hall, 2006),
315 which represents the maximum geostrophic velocity (U_{geo}) experienced on the slope (O'Neill-Baringer and Price,
316 1997). This is considerably lower than velocities observed in the region today (Sánchez-Leal et al., 2017), which are

317 $\sim 1 \text{ m s}^{-1}$ where sandy contourites are forming and in excess of 1.4 m s^{-1} in regions of abrasion (O'Neill-Baringer and
318 Price, 1999). As shown in *Results*, a low velocity MOW or AMW would directly reflect a less dense Mediterranean
319 water-mass. This implies that the Mediterranean was much less salty during the middle to late Messinian than in the
320 late Tortonian to early Messinian, which is at odds with the empirical evidence. Conceptually, some loss of density
321 could be traced to the warming of the Mediterranean relative to the Atlantic, but such a regional difference would have
322 to be unrealistically large (up to several degrees), and could still not account for the latest Miocene when halite or
323 gypsum were deposited in the Mediterranean. Moreover, a slower maximum flow velocity threshold (0.15 m s^{-1})
324 would mean a more significant reduction of salinity in the Mediterranean. Hence we find no conditions under which
325 our seismic observations are explained by a very slow-moving plume.

326 *Could the plume have moved?*

327 As the position of the gateway moved, the contourite deposition downstream of it must have moved as well.
328 The data covers the most northerly (Fig. 2a and 3b) to the most southerly gateway recognized (Fig. 2b and 3c), fully
329 capturing the possibility of a change in gateway position, thus eliminating this possibility. It might be that the MOW
330 plume moved deeper down the slope, coming to lie basinward of the seismic data presented. For the Late Quaternary,
331 such alterations have been documented (Schönfeld et al., 2003; Llave et al., 2006; Rogerson et al., 2012a). Given the
332 operations of mixing and/or entrainment to counter changes in the density of outflowing water (see discussion above),
333 such settings would not arise from changes in the Mediterranean basin itself, but rather from a weakening of the
334 Atlantic Meridional Overturning Circulation (Rogerson et al., 2012a). In order for the AMW to reach water depths
335 beyond the range of the seismic data presented here, the AMOC would have had to weaken to approximately its
336 conditions during the Last Glacial Maximum (Rogerson et al., 2005). A slow AMOC may have occurred in warm
337 periods of the Early Miocene, but there is no evidence in favour of this hypothesis for the Late Miocene
338 (Steinhorsdottir et al., 2020), and the relatively low volume of northern polar ice at the time, as compared to the Late
339 Quaternary Heinrich Events, makes a “thermohaline crisis” scenario in the Atlantic difficult to envisage. We therefore
340 do not speculate about a sustained period of very low AMOC throughout the deposition of the middle to upper
341 Messinian unit (up to several hundreds of thousands of years) in support of a deepwater flow at this time
342 (Steinhorsdottir et al., 2020). Unless such evidence of sustained low Atlantic overturning during the middle to late

343 Messinian is presented, the AMW plume could not be expected to lie lower on the slope than the region of the seismic
344 data we examined.

345 *Was the Mediterranean-Atlantic water-mass exchange different from that of today?*

346 Recent consensus regarding the evaporite-depositing phases in the latest Miocene evokes an extremely
347 stratified Mediterranean basins (Yoshimura et al., 2016), with exceptionally dense brines occupying deep areas below
348 sills connecting with the Atlantic. However, these deep brine bodies would remain within a Mediterranean overturning
349 circulation, where quantitative representations of the basin demonstrate that deep brines would have continued to mix
350 into overlying waters (Simon and Meijer, 2017), and as part of that advection were likely directly drawn up to sill
351 depth by frictional Bernoulli aspiration (Rogerson et al., 2012b). Advection of deep waters is required to balance the
352 water volume provided to finite deep basins by convection (Simon and Meijer, 2017); without the Mediterranean
353 overturning circulation, the mass of salt held in water within the deep basins could rapidly be exhausted and evaporite
354 deposition would be replaced by sapropel deposition. The extreme stratification scenarios provided by Simon and
355 Meijer (2017) are therefore consistent with the quantitative representation of the AMW plume used here, and do not
356 suffice to explain the lack of a contourite depositional system in the Gulf of Cádiz.

357 By discarding other reasonable scenarios through this hypothetico-deductive method, we find that the most
358 likely explanation for our seismic observations in the Gulf of Cádiz and the non-desiccation of the Mediterranean
359 during the deposition of the middle to upper Messinian unit is inflow-without-outflow. This implies that the interface
360 between the surficial and intermediate (e.g. LIW) water-masses in the Mediterranean had already been drawn to- or
361 below sill depth, while the Atlantic sea surface remaining above it provided continuous unidirectional eastward flow
362 of relatively fresh water into the Mediterranean, balancing evaporation. Still, we are unable to affirm whether there
363 were sporadic outflows across the Mediterranean-Atlantic gateway during the middle to upper Messinian, which may
364 be required to maintain salinity below evaporitic saturation (Roveri et al., 2014), as the primary impact would be deep
365 scouring close to the strait (Siddall et al., 2004) later masked by Pliocene erosion (Fig. 4). We likewise find no positive
366 indication of changes in seismic facies in the middle to upper Messinian unit within the seismic resolution of our
367 dataset that could account for sporadic outflows in parts of the margins with a more conformable succession (Fig. 2).
368 Further research is necessary to determine whether this period of apparently no MOW nor AMW plume activity is
369 punctuated by shorter returns to two-way water-mass exchange; or whether salt was lost from the Mediterranean basin

370 by other means, such as an earlier-than-anticipated onset of evaporite deposition in the deep Eastern Mediterranean
371 basins.

372 Implications of the Late Miocene Mediterranean-Atlantic Gateway Restriction

373 The basal unconformity of the middle to late Messinian unit (~6.4 Ma) is linked to an onset of dominantly hemipelagic
374 depositional environment. This seismic and lithologic change suggests absent or intermittent bottom currents without
375 the influence of MOW through the Late Miocene paleo-gateways before the onset of MSC evaporite precipitation and
376 deposition in the Mediterranean. The reduced MOW in the Gulf of Cádiz during the middle to late Messinian was
377 probably due to the shallowing of the sill in the paleo-gateway by tectonic uplift (Krijgsman et al., 1999). Accordingly,
378 the threshold depth allowed solely Atlantic inflow (Capella et al., 2019; Flecker et al., 2015) or intermittent outflow
379 incapable of significantly reworking sediments on the slope of the Gulf of Cádiz since at least 6.37 Ma, ~400 kyr
380 preceding the onset of the MSC (Manzi et al., 2018). This scenario is consistent with a shift from paleo-MOW to
381 paleo-Atlantic bottom waters in the Onshore Gharb basin between ~6.64 and 6.44 Ma, based on Neodymium (Nd)
382 isotope values in the Bou Regreg valley succession in the Riffian corridor (Salé Briqueterie, Ain El Beida and Oued
383 Akrech; Fig. 7; Ivanovic et al., 2013). Regional uplift and tectonism (Duggen et al., 2003) could also have driven
384 formation of the turbidites observed at the base of the middle to upper Messinian unit, with turbidite channels scouring
385 into the lower Messinian unit. The reduction of MOW we report at the ~6.4 Ma mark also coincides with a 400-kyr
386 eccentricity minima of the orbital solution by Laskar et al. (2004) (Fig. 5), and supports a stepwise nature for the
387 progressive restriction of the Mediterranean-Atlantic gateway, further consolidating the 400-kyr periodicity orbital
388 forcing superimposed on a gradual tectonic trend as the mechanism behind gateway closure (Hilgen et al., 2007) and
389 changes in the dominant depositional style. An astronomical link to the long eccentricity orbital forcing has been
390 proposed for the evolution of stratigraphic events in this region leading up to the MSC (Roveri et al., 2014), namely
391 the Tortonian Salinity Crisis (7.8–7.6 Ma) (Krijgsman et al., 2000), the stepwise restriction of Mediterranean-Atlantic
392 connection (~7.2 and ~6.8 Ma) (Kouwenhoven et al., 2003), onset of MSC (5.97 Ma) (Manzi et al., 2018), and the
393 “Messinian Gap” or MSC acme event (5.6–5.55 Ma) (Krijgsman et al., 1999). The gateway restriction, along with
394 paleoceanographic changes, could explain the concurrent phylogenetic divergence of Mediterranean-New World
395 monk seals around 6.3 Ma, similar to the effect of the Central American seaway closure on Caribbean-Hawaiian monk
396 seal divergence (Scheel et al., 2014).

397 In the Mediterranean, the gateway restriction was also recorded progressively, leading up to the weakening
398 of the MOW at ~6.4 Ma, firstly by a significant reduction of deep-water ventilation immediately after the Tortonian-
399 Messinian boundary (7.15 Ma), followed by an intensification of bottom-water stagnation and water stratification (6.7
400 Ma; Blanc-Valleron et al., 2002; Kouwenhoven et al., 1999; 2003). These changes were accompanied by a lesser
401 diversity of calcareous planktons (Sierro et al., 2003). Then, deposition of aplanktic levels related to more adverse
402 conditions of restriction with increased salinity (>50 g/L) took place since 6.4 Ma (Sierro et al., 2008). This period
403 (6.45 – 6.29 Ma) is furthermore characterized by more negative and unstable $\delta^{18}\text{O}$ values in the Mediterranean,
404 suggesting stronger dilution by continental waters, pointing to a severe isolation of the Mediterranean basin, which
405 was no longer regulated by oceanic input but by climatic fluctuations (Blanc-Valleron et al., 2002). The widespread
406 precipitation of authigenic calcite, dolomite and/or aragonite in the Mediterranean between 6.3 and 5.97 Ma, prior to
407 the deposition of MSC evaporites, moreover indicates an increasingly restrictive and supersaturated environment
408 (Blanc-Valleron et al., 2002; Sierro et al., 2003). A continuous but reduced surficial Atlantic inflow into the
409 Mediterranean could contribute to varying salinity levels around the upper tolerance limit of foraminifera (50 g/L),
410 but below the threshold of gypsum deposition (130 g/L; Flecker et al., 2015) in the Mediterranean marginal basins;
411 meanwhile, the absence of outflow to the Atlantic requires salt being lost from the Mediterranean basin through other
412 means, from the initiation of the transparent unit until the onset of MSC (~6.4 – 5.97 Ma). In the deeper basins, euxinic
413 shales in the pre-MSC interval (Roveri et al., 2014) extending into the first stage of MSC (de Lange and Krijgsman,
414 2010) indicate anoxic and sulphidic bottom water conditions that could impede the precipitation of gypsum even
415 where salinity was strongly enhanced. Reduced conditions in the deep basin would also explain the synchronous onset
416 of marginal gypsum and basinal halite precipitation, reaching saturations of 130 and 350 g/L, respectively (Meilijson
417 et al., 2018). Such a scenario still requires a sink of salt from the basin, however either via sporadic outbursts into the
418 Atlantic too subtle for seismic reflection data to resolve, or owing to an earlier-than-anticipated onset of salt deposition
419 in the deep Mediterranean basins. Either hypothesis will need to be tested via new coring and research.

420 The transition from contouritic to hemipelagic sedimentation in the Miocene would give rise to changes in
421 the Atlantic paleoceanographic regime (Fig. 6). A restricted Mediterranean-Atlantic connection and an absence or
422 intermittence of MOW during the middle to late Messinian would have significantly reduced Atlantic water
423 entrainment and halted formation of the AMW (Rogerson et al., 2012b). This would alter the strength, structure and
424 possibly the position of the Azores Front (Ozgokmen et al., 2001) and destabilize the AMOC (Ivanovic et al., 2014;

425 Pérez-Asensio et al., 2012, Sierro et al., 2020). Assuming that the buoyancy export during the early Messinian was
426 similar to that existing today, a loss of MOW would reduce the buoyancy loss within the North Atlantic by $\sim 8.53 \times$
427 10^5 kg s^{-1} , which is a change of the same magnitude as that arising from Anthropocene Arctic sea ice loss (Liu et al.,
428 2019). A unidirectional loss of salt into the Mediterranean via an inflow-without-outflow scenario at Gibraltar during
429 the Messinian would also differ from a small net inflow of salt relative to the total inflow-outflow budget under the
430 present two-way exchange scenario. This would likely result in anomalously low salinity in the adjacent Northeastern
431 Atlantic, and possibly the weakest AMOC since the closure of the connection between the Mediterranean and the
432 Indian Ocean during the middle Miocene (de la Vara et al., 2013). A revised astronomical age model for ODP Site
433 982 in the North Atlantic (Fig. 6; Drury et al., 2018), correlated to the Ain El Beida section in the Bou Regreg Valley
434 (Fig. 6; van der Laan et al., 2005) indicates benthic excursions of $\delta^{18}\text{O}$ and $\delta^{13}\text{C}$ in the Atlantic intermediate water
435 depths (500–1500 m; *sensu* Emery and Meincke, 1986) around ~ 6.4 Ma (Drury et al., 2018). The higher average $\delta^{18}\text{O}$
436 and $\delta^{13}\text{C}$ values suggest colder conditions (Drury et al., 2018) and could testify to the removal of warm and saline
437 AMW and glacial shoaling of the NADW (Gebbie, 2014; Fig. 6b). This major paleoceanographic change is responsible
438 for the enhanced subsurface and atmospheric cooling in the mid-latitudes of the Northern Hemisphere (Boulton et al.,
439 2014; Ivanovic et al., 2014), which coincides with dynamic ice sheet expansion and strengthening of the cryosphere-
440 carbon cycle coupling between 6.4 and 5.4 Ma (Drury et al., 2018; Herbert et al., 2016).

441 **Conclusions**

442 The widespread distribution of a predominantly hemipelagic middle to upper Messinian unit along the continental
443 slope in the Gulf of Cádiz and the southern part of the West Iberian margin can be viewed as the sedimentary response
444 to an absence or intermittence of intermediate circulation. This implies no continuous outflow of the Mediterranean-
445 Atlantic exchange at least ~ 400 kyr preceding the MSC, simultaneous to progressive gateway restriction, and
446 correlates to AMOC weakening and North Atlantic cooling in the latest Miocene. An alternative interpretation is that
447 the AMOC was severely reduced throughout this period, causing the MOW plume to settle at great depth. As this is
448 not consistent with existing reconstructions of the Atlantic during the Late Miocene, we support the former scenario.
449 Either as a means of explaining the transparent unit via deep settling, or as a consequence of inflow-without-outflow
450 causing major palaeoceanographic changes throughout the North Atlantic, the evolution of the Mediterranean at this
451 time seems to be inextricably bound to the evolution of AMOC. One important outcome of this study is the recognition

452 of the disadvantages of considering the two basins in isolation, and of the need to integrate conceptual models of
453 Atlantic paleoceanography with Mediterranean geological models for the latest Miocene.

454 **Acknowledgments and Data**

455 The authors would like to thank the editor and two anonymous reviewers for their constructive comments. This work
456 is conducted in the framework of “*The Drifters*” *Research Group*, Royal Holloway University of London, and
457 supported by Royal Holloway college studentship, SCORE (CGL2016-80445-R) and INPULSE (CTM2016-75129-
458 C3-1-R) projects. The authors would also like to extend their grateful thanks to Mr. Mohamed Nahim as Director of
459 Petroleum Exploration (ONHYM) for his support, and to ONHYM, Repsol S.A., and TGS-Nopec for permission to
460 use the seismic and borehole data in this work. Datasets for this research are partly included in the literature
461 (Hernández-Molina et al., 2014; 2016; Ledesma, 2000; van der Schee et al., 2016), and partly available from ONHYM,
462 Repsol S.A., and TGS-Nopec with confidentiality regulations, and are not publicly accessible, but are available from
463 the authors upon reasonable request and with permissions of ONHYM, Repsol S.A., and TGS-Nopec.

464 **References**

465 Berggren, W.A. (1982). Role of Ocean Gateways in Climate Change. In: Climate in Earth History. *Studies in*
466 *Geophysics*, 118-125. Washington D.C.: National Academy Press.

467 Bethoux, J. P., & Gentili, B. (1999). Functioning of the Mediterranean Sea: past and present changes related to
468 freshwater input and climate changes. *Journal of Marine Systems*, 20, 33-47. doi:10.1016/S0924-7963(98)00069-4

469 Blanc-Valleron, M.-M., Pierre, C., Caulet, J. P., Caruso, A., Rouchy, J.-M., Cespuglio, G., Sprovieri, R., Pestrea, S.,
470 & Di Stefano, E. (2002). Sedimentary, stable isotope and micropaleontological records of paleoceanographic change
471 in the Messinian Tripoli Formation (Sicily, Italy). *Palaeogeography, Palaeoclimatology, Palaeoecology* 185, 255-
472 286. doi:10.1016/S0031-0182(02)00302-4

473 Boulton, C. A., Allison, L. C., & Lenton T. M. (2014). Early warning signals of Atlantic Meridional Overturning
474 Circulation collapse in a fully coupled climate model. *Nature Communications* 5, 5752. doi:10.1038/ncomms6752

475 Bryden, L. H. (1993). Sill exchange to and from enclosed seas. In N. F. R. Delia Croce (Ed.), *Symposium*
476 *Mediterranean Seas 2000*, Università di Genova, Santa Margherita Ligure, 23–27 September 1991 (pp. 17-41)
477 Genova: Istituto Scienze Ambientali Marine.

478 Capella, W., Flecker, R., Hernández-Molina, F. J., Simon, D., Meijer, P. T., Rogerson, M., Sierro, F. J., &
479 Krijgsman, W. (2019). Mediterranean isolation preconditioning the Earth System for late Miocene climate cooling.
480 *Scientific Reports*, 9, 3795. doi:10.1038/s41598-019-40208-2

481 Capella, W., Hernández-Molina, F. J., Flecker, R., Hilgen, F. J., Hssain, M., Kouwenhoven, T. J., van Oorschot,
482 M., Sierro, F. J., Stow, D. A. V., Trabucho-Alexandre, J., Tulbure, M. A., de Weger, W., Yousfi, M. Z., &
483 Krijgsman, W. (2017). Sandy contourite drift in the late Miocene Rifian Corridor (Morocco): reconstruction of
484 depositional environments in a foreland-basin seaway. *Sedimentary Geology*, 355, 31–57.
485 doi:10.1016/j.sedgeo.2017.04.004

486 Culp, J., Strom, K., Parent, A., & Romans, B. W. (2020). Sorting of fine-grained sediment by currents: Testing the
487 sortable silt hypothesis with laboratory experiments. *Earth Arxiv*. doi:10.31223/osf.io/xec2t [Accessed
488 31/12/2020].

489 de la Vara, A., Meijer, P. Th., & Wortel, M. J. R. (2013). Model study of the circulation of the Miocene Mediterranean
490 Sea and Paratethys: closure of the Indian Gateway. *Climate of the Past Discussion*, 9, 4385-4424. doi:10.5194/cpd-9-
491 4385-2013

492 de Lange, G. J., & Krijgsman, W. (2010). Messinian salinity crisis: A novel unifying shallow gypsum/deep dolomite
493 formation mechanism. *Marine Geology*, 275, 273–277. doi:10.1016/j.margeo.2010.05.003

494 de Weger, W., Hernández-Molina, F. J., Flecker, R., Sierro, F. J., Chiarella, D., Krijgsman, W. & Manar, M. A.
495 (2020). Late Miocene contourite channel system reveals intermittent overflow behavior. *Geology*.
496 doi:10.1130/G47944.1

497 Drury, A. J., Westerhold, T., Hodell, D., & Röhl, U. (2018). Reinforcing the North Atlantic backbone: revision and
498 extension of the composite splice at ODP Site 982. *Climate of the Past*, 14, 321-338. doi:10.5194/cp-14-321-2018

499 Ducassou, E., Fournier, L., Sierro, F. J., Alvarez Zarikian, C. A., Lofi, J., Flores, J. A., & Roque, C. (2016).
500 Origin of the large Pliocene and Pleistocene debris flows on the Algarve margin. *Marine Geology*, 377, 58-76.
501 doi:10.1016/j.margeo.2015.08.018

502 Duggen, S., Hoernle, K., van den Bogaard, P., Rüpke, L., & Morgan, J. P. (2003). Deep roots of the Messinian salinity
503 crisis. *Nature*, 422, 602-606. doi:10.1038/nature01551

504 Emery, W. J., & Meincke, J. (1986). Global Water Masses: Summary and Review. *Oceanologica Acta*, 9, 383-391.

505 Flecker, R. & Ellam, R.M. (2006). Identifying Late Miocene episodes of connection and isolation in the
506 Mediterranean–Paratethyan realm using Sr isotopes. *Sedimentary Geology* 188-189, 189-203.
507 doi:10.1016/j.sedgeo.2006.03.005

508 Flecker, R., Krijgsman, W., Capella, W., de Castro Martíns, C., Dmitrieva, E., Mayser, J. P., Marzocchi, A., Modestou,
509 S., Ochoa, D., Simon, D., Tulbure, M., van den Berg, B., van der Schee, M., de Lange, G., Ellam, R., Govers, R.,
510 Gutjahr, M., Hilgen, F. J., Kouwenhoven, T., Lofi, J., Meijer, P., Sierro, F. J., Bachiri, N., Barhoun, N., Chakor Alami,
511 A., Chacon, B., Flores, J. A., Gregory, J., Howard, J., Lunt, D., Ochoa, M., Pancost, R., Vincent, S., & Zakaria Yousfi,
512 M. (2015). Evolution of the Late Miocene Mediterranean-Atlantic gateways and their impact on regional and global
513 environmental change. *Earth-Science Reviews* 150, 365-392. doi:10.1016/j.earscirev.2015.08.007

514 Gebbie, G. (2014). How much did Glacial North Atlantic Water shoal? *Paleoceanography*, 29, 190-209.
515 doi:10.1002/2013PA002557

516 Henrich R., & Hüneke, H. (2011). Hemipelagic Advection and Periplatform Sedimentation. In: H. Hüneke, & T.
517 Mulder (Eds.), Deep-sea Sediments. *Developments in Sedimentology*, 63, 353-396. doi:10.1016/B978-0-444-53000-
518 4.00005-6

519 Herbert, T. D., Lawrence, K. T., Tzanova, A., Peterson, L. C., Caballero-Gill, R., & Kelly, C.S. (2016). Late
520 Miocene global cooling and the rise of modern ecosystems. *Nature Geoscience*, 9, 843–847. doi:10.1038/ngeo2813

521 Hernández-Molina, F. J., Llave, E., Preu, B., Ercilla, G., Fontan, A., Bruno, M., Serra, N., Gomiz, J. J., Brackenridge,
522 R. E., Sierro, F. J., Stow, D. A. V., García, M., Juan, C., Sandoval, N., & Arnáiz, A. (2014). Contourite processes

523 associated with the Mediterranean Outflow water after its exit from the Strait of Gibraltar: global and conceptual
524 implications. *Geology*, 42, 227–230. doi:10.1130/G35083.1

525 Hernández-Molina, F. J., Sierro, F. J., Llave, E., Roque, C., Stow, D. A. V., Williams, T., Lofi, J., van der Schee, M.,
526 Arnáiz, A., Ledesma, S., Rosales, C., Rodríguez-Tovar, F. J., Pardo-Igúzquiza, E., & Brackenridge, R. E. (2016).
527 Evolution of the gulf of Cádiz margin and southwest Portugal contourite depositional system: Tectonic, sedimentary
528 and paleoceanographic implications from IODP expedition 339. *Marine Geology* 377, 7-39.
529 doi:10.1016/j.margeo.2015.09.013

530 Hilgen, F. J., Krijgsman, W., Langereis, C. G., Lourens, L. J., Santarelli, A., & Zachariasse, W. J. (1995). Extending
531 the astronomical (polarity) time scale into the Miocene. *Earth Planetary Science Letters* 136, 495-510.
532 doi:10.1016/0012-821X(95)00207-S

533 Hilgen, F., Kuiper, K., Krijgsman, W., Snel, E., & van der Laan, E. (2007). Astronomical tuning as the basis for high
534 resolution chronostratigraphy: the intricate history of the Messinian Salinity Crisis. *Stratigraphy* 4, 231-238.

535 Hodell, D. A., Curtis, J. H., Sierro, F. J., & Raymo, M. E., (2001). Correlation of late Miocene to early Pliocene
536 sequences between the Mediterranean and North Atlantic. *Palaeoceanography* 16, 164–178.
537 doi:10.1029/1999PA000487

538 Hüsing, S. K., Oms, O., Agustí, J., Garcés, M., Kouwenhoven, T. J., Krijgsman, W., & Zachariasse, W.-J. (2010). On
539 the late Miocene closure of the Mediterranean–Atlantic gateway through the Guadix basin (southern Spain).
540 *Palaeogeography, Palaeoclimatology, Palaeoecology* 291, 167–179. doi:10.1016/j.palaeo.2010.02.005.

541 Iaccarino, S. M., Cita, M. B., Gaboardi, S., & Gruppini, G. M. (1999). High-resolution biostratigraphy at the
542 Miocene/Pliocene boundary in Holes 974B and 975B, western Mediterranean. *Proceedings of the Ocean Drilling*
543 *Program, Scientific Results* 161 (pp. 197–221). College Station, TX: Ocean Drilling Program.
544 doi:10.2973/odp.proc.sr.161.247.1999

545 Ivanovic, R. F., Flecker, R., Gutjahr, M., & Valdesa, P. J. (2013). First Nd isotope record of Mediterranean–Atlantic
546 water exchange through the Moroccan Rifian Corridor during the Messinian Salinity Crisis. *Earth Planetary Science*
547 *Letters*, 368, 163-174. doi:10.1016/j.epsl.2013.03.010

548 Ivanovic, R. F., Valdes, P. J., Flecker, R., & Gutjahr, M. (2014). Modelling global-scale climate impacts of the late
549 Miocene Messinian Salinity Crisis. *Climate of the Past*, 10, 607-622. doi:10.5194/cp-10-607-2014

550 Knutz, P.C. (2008). Paleooceanographic significance of contourite drifts. In: M. Rebesco & A. Camerlenghi (Eds.),
551 Contourites. *Developments in Sedimentology*, 60, 511-535. Amsterdam: Elsevier.

552 Kouwenhoven, T. J., Seidenkrantz, M.-S. & van der Zwaana, G. J. (1999). Deep-water changes: the near-synchronous
553 disappearance of a group of benthic foraminifera from the Late Miocene Mediterranean. *Palaeogeography*,
554 *Palaeoclimatology, Palaeoecology* 152, 259-281. doi:10.1016/S0031-0182(99)00065-6

555 Kouwenhoven, T. J., Hilgen, F. J., & van der Zwaan, G. J. (2003). Late Tortonian-early Messinian stepwise disruption
556 of the Mediterranean-Atlantic connections: constraints from benthic foraminiferal and geochemical data.
557 *Palaeogeography Palaeoclimatology Palaeoecology*, 198, 303-319. doi:10.1016/S0031-0182(03)00472-3

558 Krijgsman, W., Capella, W., Simon, D., Hilgen, F. J., Kouwenhoven, T. J., Meijer, P. Th., Sierro, F. J., Tubbare, M.
559 A., van den Berg, B. C. J., van der Schee, M., & Flecker, R. (2018). The Gibraltar Corridor: Watergate of the Messinian
560 Salinity Crisis. *Marine Geology*, 403, 238-246. doi:10.1016/j.margeo.2018.06.008

561 Krijgsman, W., Gaboardi, S., Hilgen, F. J., Iaccarino, S., de Kaenel, E., & van der Laan, E. (2004). Revised
562 astrochronology for the Ain el Beida section (Atlantic Morocco): No glacio-eustatic control for the onset of the
563 Messinian Salinity Crisis. *Stratigraphy*, 1, 87-101.

564 Krijgsman, W., Garcés, M., Agustí, J., Raffi, I., Taberner, C., & Zachariasse, W. J. (2000). The 'Tortonian salinity
565 crisis' of the eastern Betics (Spain). *Earth Planetary Science Letters*, 181, 497-51. doi:10.1016/S0012-
566 821X(00)00224-7

567 Krijgsman, W., Hilgen, F. J., Raffi, I., Sierro, F. J., & Wilson, D. S. (1999). Chronology, causes and progression of the
568 Messinian salinity crisis. *Nature*, 400, 652-655. doi:10.1038/23231

569 Laskar, J., Robutel, P., Joutel, F., Gastineau, M, Correia, A. C. M., & Levrard., B. (2004). A long-term numerical
570 solution for the insolation quantities of the Earth. *Astronomy and Astrophysics* 428, 261-285. doi:10.1051/0004-
571 6361:20041335

572 Ledesma, S. (2000). Astrobocronología y estratigrafía de alta resolución del Neógeno de la Cuenca del Guadalquivir-
573 Golfo De Cádiz, (Doctoral dissertation). Retrieved from Grupo de Geociencias Oceánicas. ([http://oceano.usal.es/wp-](http://oceano.usal.es/wp-content/uploads/sites/30/2017/10/SantiagoLedesmaTesis.compressed-1.pdf)
574 [content/uploads/sites/30/2017/10/SantiagoLedesmaTesis.compressed-1.pdf](http://oceano.usal.es/wp-content/uploads/sites/30/2017/10/SantiagoLedesmaTesis.compressed-1.pdf)). Salamanca: Universidad de Salamanca.

575 Liu, W., Fedorov, A., & Sévellec, F. (2019). The Mechanisms of the Atlantic Meridional Overturning Circulation
576 Slowdown Induced by Arctic Sea Ice Decline. *Journal of Climate*, *32*, 977-996. doi:10.1175/JCLI-D-18-0231.1

577 Liu, W., Fedorov, A., Xie, S.-P., & Hu, S. (2020). Climate impacts of a weakened Atlantic Meridional Overturning
578 Circulation in a warming climate. *Science Advances*, *6*, eaaz4876. doi:10.1126/sciadv.aaz4876

579 Llave, E., Schönfeld, J., Hernández-Molina, F. J., Mulder, T., Somoza, L., Díaz del Río, V., & Sánchez-Almazo, I.
580 (2006). High-resolution stratigraphy of the Mediterranean outflow contourite system in the Gulf of Cadiz during the
581 late Pleistocene: The impact of Heinrich events. *Marine Geology*, *227*, 241 – 262. doi:10.1016/j.margeo.2005.11.015

582 Lopes, F. C., Cunha, P. P., & Le Gall, B. (2006). Cenozoic seismic stratigraphy and tectonic evolution of the Algarve
583 margin (offshore Portugal, southwestern Iberian Peninsula). *Marine Geology*, *231*, 1-36.
584 doi:10.1016/j.margeo.2006.05.007

585 Lourens, L. J., Antonarakou, A., Hilgen, F. J., Van Hoof, A. A. M., Vergnaud-Grazzini, C., & Zachariasse, W. J.
586 (1996). Evaluation of the Plio-Pleistocene astronomical timescale. *Paleoceanography*, *11*, 391-413.
587 doi:10.1029/96PA01125

588 Lourens, L. J., Hilgen, F. J., Shackleton, J., Laskar, J., & Wilson, J. (2004). The Neogene Period. In: F. Gradstein, J.
589 Ogg, & A. Simth (Eds.), *A Geologic Time Scale*, 409–440. London: Cambridge University Press.

590 Maldonado, A., Somoza, L., & Pallarés, L., (1999). The Betic orogen and the Iberian-African boundary in the Gulf of
591 Cádiz: geological evolution (central North Atlantic). *Marine Geology*, *155*, 9-43. doi:10.1016/S0025-3227(98)00139-
592 X

593 Manzi, V., Gennari, R., Lugli, S., Persico, D., Reghizzi, M., Roveri, M., Schreiber, B. C., Calvo, R., Gavrieli, I., &
594 Gvirtzman, Z. (2018). The onset of the Messinian salinity crisis in the deep Eastern Mediterranean basin. *Terra Nova*,
595 *30*, 189-198. doi:10.1111/ter.12325

596 Martín, J. M., Braga, J. C. & Betzler, C. (2002). The Messinian Guadalhorce corridor: the last northern, Atlantic–
597 Mediterranean gateway. *Terra Nova* 13, 418-424. doi:10.1046/j.1365-3121.2001.00376.x

598 Martín, J. M., Braga, J. C., Aguirre, J., & Puga-Bernabéu, Á. (2009). History and evolution of the North-Betic Strait
599 (Prebetic Zone, Betic Cordillera): A narrow, early Tortonian, tidal-dominated, Atlantic-Mediterranean marine
600 passage. *Sedimentary Geology*, 216, 80-90. doi:10.1016/j.sedgeo.2009.01.005

601 McCave, I. N., & Hall, I. R. (2006), Size sorting in marine muds: Processes, pitfalls, and prospects for paleoflow-
602 speed proxies. *Geochemistry, Geophysics, Geosystems*, 7, Q10N05, doi:10.1029/2006GC001284.

603 McCave, I. N., Thornalley, D. J. R., & Hall, I. R. (2017). Relation of sortable silt grain-size to deep-sea current speeds:
604 Calibration of the ‘Mud Current Meter’. *Deep Sea Research Part I: Oceanographic Research Papers*, 127, 1-12.
605 doi:10.1016/j.dsr.2017.07.003

606 Medialdea, T., Vegas, R., Somoza, L., Vázquez, J. T., Maldonado, A., Díaz-del-Río, V., Maestro, A., Córdoba, D., &
607 Fernández-Puga, M. C., (2004). Structure and evolution of the “Olistostrome” complex of the Gibraltar Arc in the
608 Gulf of Cádiz (eastern Central Atlantic): evidence from two long seismic cross-sections. *Marine Geology* 209, 173-
609 198. doi:10.1016/j.margeo.2004.05.029

610 Meijer, P. Th. & Krijgsman, W. (2005). A quantitative analysis of the desiccation and re-filling of the Mediterranean
611 during the Messinian Salinity Crisis. *Earth and Planetary Science Letters* 240, 510 – 520.
612 doi:10.1016/j.epsl.2005.09.029

613 Meilijson, A., Steinberg, J., Hilgen, F. J., Bialik, O. M., Waldmann, N. D., & Makovsky, Y. (2018). Deep-basin
614 evidence resolves a 50-year-old debate and demonstrates synchronous onset of Messinian evaporite deposition in a
615 non-desiccated Mediterranean. *Geology*, 46, 243–246. doi:10.1130/G39868.1

616 Millot, C., Candela, J., Fuda, J.-L., & Tber, Y. (2006). Large warming and salinification of the Mediterranean outflow
617 due to changes in its composition. *Deep Sea Research Part I: Oceanographic Research Papers*, 53, 656-666.
618 doi:10.1016/j.dsr.2005.12.017

619 O'Neill-Baringer, M., & Price, J. F. (1997). Mixing and spreading of the Mediterranean outflow. *Journal of Physical*
620 *Oceanography*, 27, 1654-1677. doi:10.1175/1520-0485(1997)027<1654:MASOTM>2.0.CO;2

621 O'Neill-Baringer, M. & Price, J. F. (1999). A review of the physical oceanography of the Mediterranean outflow.
622 *Marine Geology*, 155, 63-82. doi:10.1016/S0025-3227(98)00141-8

623 Ozgokmen, T. M., Chassignet, E. P., & Rooth, C. G. H. (2001). On the connection between the Mediterranean Outflow
624 and the Azores current. *Journal of Physical Oceanography*, 31, 461-480. doi:10.1175/1520-
625 0485(2001)031<0461:OTCBTM>2.0.CO;2

626 Pérez-Asensio, J. N., Aguirre, J., Schmiedl, G., & Civis, J. (2012). Impact of restriction of the Atlantic-Mediterranean
627 gateway on the Mediterranean Outflow Water and eastern Atlantic circulation during the Messinian.
628 *Paleoceanography*, 27, PA3222. doi:10.1029/2012PA002309

629 Pérez-Asensio, J. N., Larrasoaña, J. C., Samankassou, E. Sierro, F. J., García Castellanos, D., Jiménez-Moreno, G.,
630 Salazar, Á., Salvany i Duran, J. M., Ledesma, S., Mata, M. P., Civis, J., & Mediavilla, C. (2018).
631 Magnetobiochronology of Lower Pliocene marine sediments from the lower Guadalquivir basin: Insights into the
632 tectonic evolution of the Strait of Gibraltar area. *Geological Society of America Bulletin*, 130, 1791-1808.
633 doi:10.1130/B31892.1

634 Prather, B. E., Booth, J. R., Steffens, G. S., & Craig, P. A. (1998). Classification, Lithologic Calibration, and
635 Stratigraphic Succession of Seismic Facies of Intraslope basins, Deep-Water Gulf of Mexico. *AAPG Bulletin* 82, 701–
636 728. doi:10.1306/1D9BC5D9-172D-11D7-8645000102C1865D

637 Riaza, C., & Martínez del Olmo, W. (1996). Depositional model of the Guadalquivir – Gulf of Cádiz Tertiary basin.
638 In P. F. Friend, & C. J. Dabrio (Eds), *Tertiary basins of Spain: The Stratigraphic Record of Crustal Kinematics* (pp.
639 330-338). Cambridge: Cambridge University Press. doi:10.1017/CBO9780511524851

640 Rodrigues, S. M. (2017). Seismostratigraphic model of the Sines Contourite Drift (SW Portuguese margin) –
641 depositional evolution, structural control and paleoceanographic implications. (Master's thesis.) Retrieved from
642 Repositório da Universidade de Lisboa. (<http://hdl.handle.net/10451/27603>). Lisbon: Universidade de Lisboa.

643 Rogerson, M., Bigg, G. R., Rohling, E., & Ramirez, J. (2012a). Vertical density gradient in the eastern North Atlantic
644 during the last 30,000 years. *Climate Dynamics* 39, 589-598. doi:10.1007/s00382-011-1148-4

645 Rogerson, M., Rohling, E. J., Bigg, G. R., & Ramirez, J. (2012b). Palaeoceanography of the Atlantic-Mediterranean
646 Exchange: Overview and first quantitative assessment of climatic forcing. *Reviews of Geophysics*, 50, RG2003.
647 doi:10.1029/2011RG000376

648 Rogerson, M., Rohling, E. J., Weaver, P. P. E., & Murray, J. W. (2004). The Azores Front since the Last Glacial
649 Maximum. *Earth and Planetary Science Letters*, 222, 779-789. doi:10.1016/j.epsl.2004.03.039

650 Rogerson, M., Rohling, E. J., Weaver, P. P. E., & Murray, J. W. (2005). Glacial to Interglacial Changes in the Settling
651 Depth of the Mediterranean Outflow Plume. *Paleoceanography*, 20, PA3007. doi:10.1029/2004PA001106

652 Roque, C. (2007). Tectonostratigrafia Do Cenozóico Das Margens Continentais Sul E Sudoeste Portuguesas: Um
653 Modelo De Correlação Sismostratigráfica. (Doctoral dissertation.) Retrieved from Repositório da Universidade de
654 Lisboa. (<http://hdl.handle.net/10451/1521>). Lisbon: Universidade de Lisboa.

655 Roveri, M., Flecker, R., Krijgsman, W., Lofi, J., Lugli, S., Manzi, V., Sierro, F. J., Bertini, A., Camerlenghi, A., De
656 Lange, G., Govers, R., Hilgen, F. J., Hübscher, C., Meijer, P. Th., & Stoica, M. (2014). The Messinian Salinity Crisis:
657 Past and future of a great challenge for marine sciences. *Marine Geology*, 352, 25-58.
658 doi:10.1016/j.margeo.2014.02.002

659 Sánchez-Leal, R. F., Bellanco, M. J., Fernández-Salas, L. M., García-Lafuente, J., Gasser-Rubinat, M., González-
660 Pola, C., Hernández-Molina, F. J., Pelegrí, J. L., Peliz, A., Relvas, P., Roque, D., Ruiz-Villarreal, M., Sammartino, S.,
661 & Sánchez-Garrido, J. C. (2017). The Mediterranean Overflow in the Gulf of Cadiz: A rugged journey. *Science*
662 *Advances*, 3, eaao0609. doi:10.1126/sciadv.aao0609

663 Scheel, D. M., Slater, G. J., Kolokotronis S. -O., Potter, C. W., Rotstein, D. S., Tsangaras, K., Greenwood A. D., &
664 Helgen, K.M. (2014). Biogeography and taxonomy of extinct and endangered monk seals illuminated by ancient DNA
665 and skull morphology. *ZooKeys*, 409, 1-33. doi:10.3897/zookeys.409.6244

666 Schönfeld, J., Zahn, R., & Abreu, L. (2003). Surface and deep water response to rapid climate changes at the Western
667 Iberian Margin. *Global and Planetary Change*, 36, 237 – 264. doi:10.1016/S0921-8181(02)00197-2

668 Scotese, C. R. (2014). Atlas of Neogene Paleogeographic Maps (Mollweide Projection). In: *PALEOMAP Atlas for*
669 *ArcGIS, Volume 1, The Cenozoic* (Maps No. 1-7). Evanston, IL: PALEOMAP Project. doi:10.13140/2.1.4151.3922

670 Selli, R., (1960). Il Messiniano Mayer-Eymar 1867. Proposta di un neostratotipo. *Giornale di Geologia* 28, 1–33. In:
671 Roveri, M., Flecker, R., Krijgsman, W., Lofi, J., Lugli, S., Manzi, V., Sierro, F. J., Bertini, A., Camerlenghi, A., De
672 Lange, G., Govers, R., Hilgen, F. J., Hübscher, C., Meijer, P. Th., & Stoica, M. (2014). The Messinian Salinity Crisis:
673 Past and future of a great challenge for marine sciences. *Marine Geology*, 352, 25-58.
674 doi:10.1016/j.margeo.2014.02.002

675 Siddall, M., Pratt, L. J., Helfrich, K. R., & Giosan, L. (2004). Testing the physical oceanographic implications of the
676 suggested sudden Black Sea infill 8400 years ago. *Paleoceanography*, 19, PA1024. doi:10.1029/2003PA000903

677 Sierro, F. J., Flores, J. A., Francés, G., Vazquez, A., Utrilla, R., Zamarreño, I., Erlenkeuser, H., & Barcena, M. A.
678 (2003). Orbitally-controlled oscillations in planktic communities and cyclic changes in western Mediterranean
679 hydrography during the Messinian. *Palaeogeography Palaeoclimatology Palaeoecology*, 190, 289-316.
680 doi:10.1016/S0031-0182(02)00611-9

681 Sierro, F. J., González Delgado, J. A., Dabrio, C. J., Flores, J. A., & Civis, J., (1996). Late Neogene depositional
682 sequences in the foreland basin of Guadalquivir (SW Spain). In P. F. Friend & C. J. Dabrio (Eds), *Tertiary basins of*
683 *Spain: The Stratigraphic Record of Crustal Kinematics* (pp.339-345). Cambridge: Cambridge University Press.
684 doi:10.1017/CBO9780511524851.048

685 Sierro, F. J., Hilgen, F. J., Krijgsman, W., & Flores, J. A. (2001). The Abad composite (SE Spain): A Mediterranean
686 and global reference section for the Messinian. *Palaeogeography Palaeoecology Palaeoclimatology*, 168, 141-169.
687 doi:10.1016/S0031-0182(00)00253-4

688 Sierro F. J., Hodell, D. A., Andersen, N., Azibeiro, L., A., Jimenez-Espejo, F. J., Bahr, A., Flores, J. A., Ausin, B.,
689 Rogerson, M., Lozano-Luz, R., Lebreiro, S. M., & Hernandez-Molina, F. J. (2020). Mediterranean Overflow Over the

690 Last 250 kyr: Freshwater Forcing From the Tropics to the Ice Sheets. *Paleoceanography and Paleoclimatology* 35.
691 doi:10.1029/2020PA003931

692 Sierro, F. J., Ledesma, S., & Flores, J. A. (2008). Astrobiochronology of Late Neogene deposits near the Strait of
693 Gibraltar (SW Spain): Implications for the tectonic control of the Messinian Salinity Crisis. In F. Briand (Ed.), *The*
694 *Messinian Salinity Crisis from mega-deposits to microbiology - A consensus report: N° 33 in CIESM Workshop*
695 *Monographs* (pp. 45-48). Monaco: CIESM Publisher.

696 Sierro, F. J., Ledesma, S., Flores, J. A., Torrecusa, S., & Martínez del Olmo, W. (2000). Sonic and gamma ray
697 astrochronology: Cycle to cycle calibration of Atlantic climatic records to Mediterranean sapropels and astronomical
698 oscillations. *Geology*, 28, 695-698. doi:10.1130/0091-7613(2000)28<695:SAGACT>2.0.CO;2

699 Simon, D., & Meijer, P. Th. (2015). Dimensions of the Atlantic–Mediterranean connection that caused the Messinian
700 Salinity Crisis. *Marine Geology*, 364, 53-64. doi:10.1016/j.margeo.2015.02.004

701 Simon, D., & Meijer, P. Th. (2017). Salinity stratification of the Mediterranean Sea during the Messinian crisis: A
702 first model analysis. *Earth and Planetary Science Letters*, 479, 366-376. doi:10.1016/j.epsl.2017.09.045

703 Steinthorsdottir, M., Coxall, H. K., De Boer, A. M., Huber, M., Barbolini, N., Bradshaw, C. D., Burls, N. J., Feakins,
704 S. J., Gasson, E., Henderiks, J., Holbourn, A., Kiel, S., Kohn, M. J., Knorr, G., Kürschner, W. M., Lear, C. H.,
705 Liebrand, D., Lunt, D. J., Mörs, T., Pearson, P. N., Pound, M. J., Stoll, H., & Strömberg, C. A. E. (2020). The Miocene:
706 the Future of the Past. *Paleoceanography and Paleoclimatology*, e2020PA004037.

707 Straume, E.O., Gaina, C., Medvedev, S., & Nisancioglu, K.H. (2020). Global Cenozoic Paleobathymetry with a focus
708 on the Northern Hemisphere Oceanic Gateways. *Gondwana Research*, 86, 126-143. doi:10.1016/j.gr.2020.05.011.

709 van der Laan, E., Gaboardi, S., Hilgen, F. J. & Lourens, L. J. (2005). Regional climate and glacial control on high-
710 resolution oxygen isotope records from Ain El Beida (latest Miocene, NW Morocco): A cyclostratigraphic analysis in
711 the depth and time domain. *Paleoceanography* 20, PA1001. doi:10.1029/2003PA000995

712 van der Laan, E., Snel, E., de Kaenel, E., Hilgen, F. J., & Krijgsman, W. (2006). No major deglaciation across the
713 Miocene–Pliocene boundary: integrated stratigraphy and astronomical tuning of the Loulja sections (Bou Regreg area,
714 NW Morocco). *Paleoceanography*, *21*, 1–27. doi:10.1029/2005PA001193

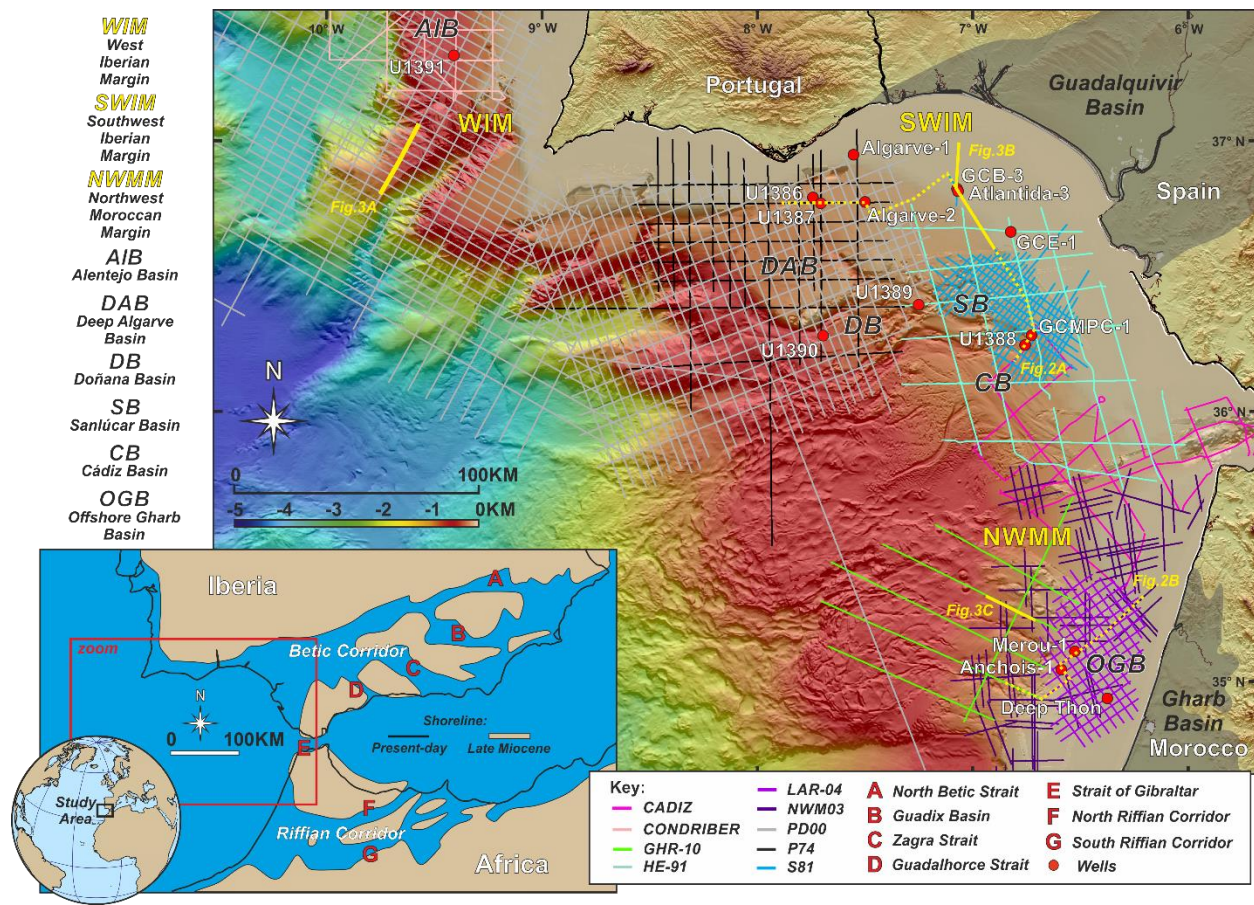
715 van der Schee, M., Sierro, F., Jimenez-Espejo, F., Hernández-Molina, F., Flecker, R., Flores, J., Acton, G.,
716 Gutjahr, M., Grunert, P., García-Gallardo, A., & Andersen, N. (2016). Evidence of early bottom water current flow
717 after the Messinian Salinity Crisis in the Gulf of Cádiz. *Marine Geology*, *380*, 315-329.
718 doi:10.1016/j.margeo.2016.04.005

719 Wüst, G. (1961). On the vertical circulation of the Mediterranean Sea. *Journal of Geophysical Research*, *66*, 3261–
720 3271. doi:10.1029/JZ066i010p03261.

721 Wynn R.B., Cronin B.T., Peakall J. (2007). Sinuous deep-water channels: Genesis, geometry and architecture. *Marine*
722 *and Petroleum Geology* *24*, 341–387. doi:10.1016/j.marpetgeo.2007.06.001

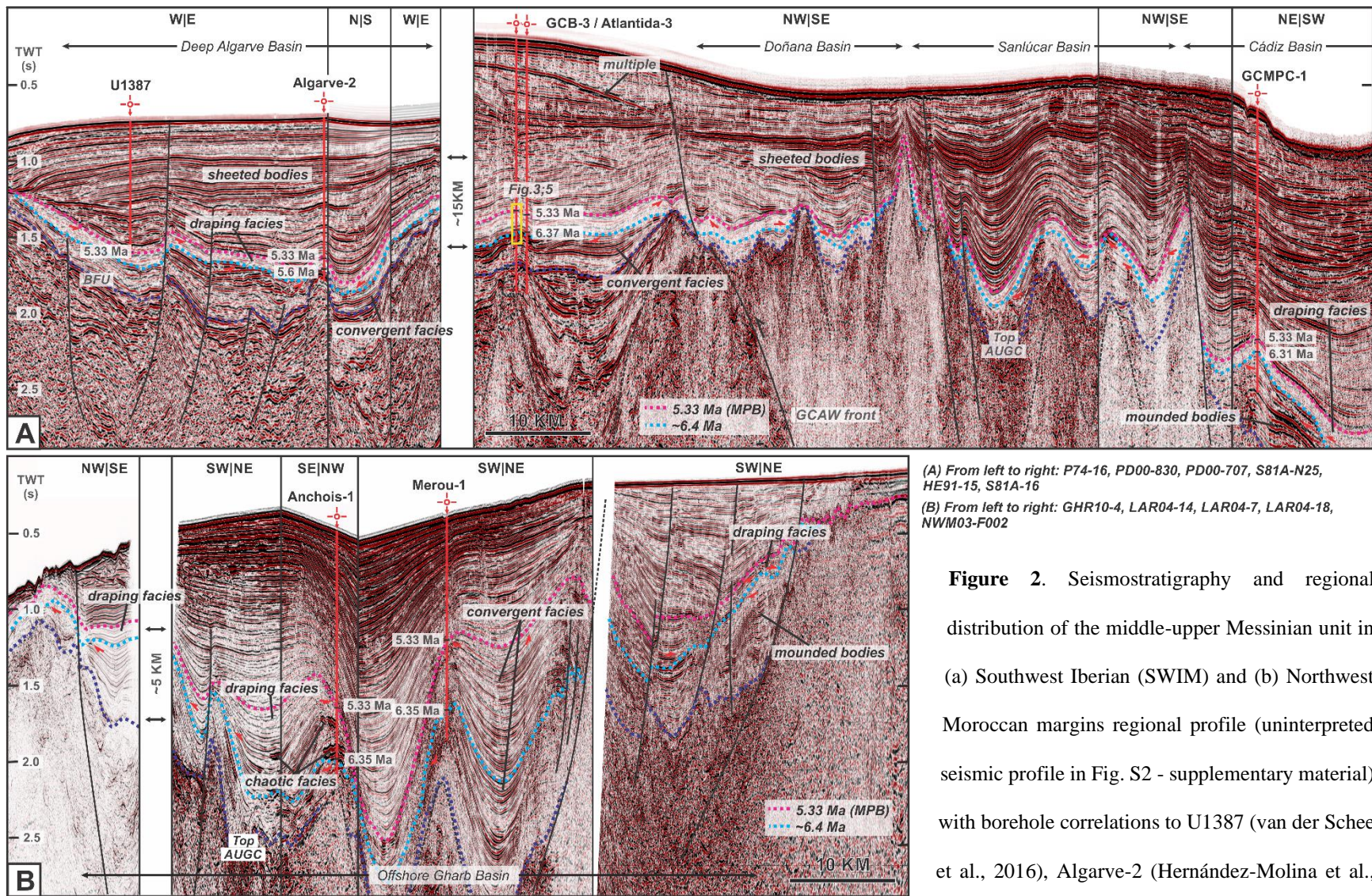
723 Yoshimura, T., Kuroda, J., Lugli, S., Tamenori, Y., Ogawa, N. O., Jiménez-Espejo, F. J., Isaji, Y., Roveri, M., Manzi,
724 V., & Kawahata, H. (2016). An X-ray spectroscopic perspective on Messinian evaporite from Sicily: Sedimentary
725 fabrics, element distributions, and chemical environments of S and Mg. *Geochemistry, Geophysics, Geosystems*, *17*,
726 1383-1400.

727 Zickfeld, K., Eby, M., & Weaver, A. J. (2008). Carbon-cycle feedbacks of changes in the Atlantic meridional
728 overturning circulation under future atmospheric CO₂. *Global Biogeochemical Cycles*, *22*, GB3024.
729 doi:10.1029/2007GB003118



730

731 **Figure 1.** Data set including post-stack, time-migrated multichannel two-dimensional (2-D) seismic reflection
 732 surveys from ONHYM, Repsol S.A., and TGS-Nopec; borehole data from exploration wells and IODP Expedition
 733 339 scientific sites. Coordinate system: WGS 84 UTM 29N. (Inset) Geographic location of the Gulf of Cádiz and
 734 the Late Miocene and present-day gateways.



(A) From left to right: P74-16, PD00-830, PD00-707, S81A-N25, HE91-15, S81A-16
 (B) From left to right: GHR10-4, LAR04-14, LAR04-7, LAR04-18, NWM03-F002

Figure 2. Seismostratigraphy and regional distribution of the middle-upper Messinian unit in (a) Southwest Iberian (SWIM) and (b) Northwest Moroccan margins regional profile (uninterpreted seismic profile in Fig. S2 - supplementary material) with borehole correlations to U1387 (van der Schree et al., 2016), Algarve-2 (Hernández-Molina et al., 2016), Atlantida-3 and GCB-3 (Ledesma, 2000), and

GCMPC-1 (Hernández-Molina et al., 2014) (Table S1 in *supplementary material*).

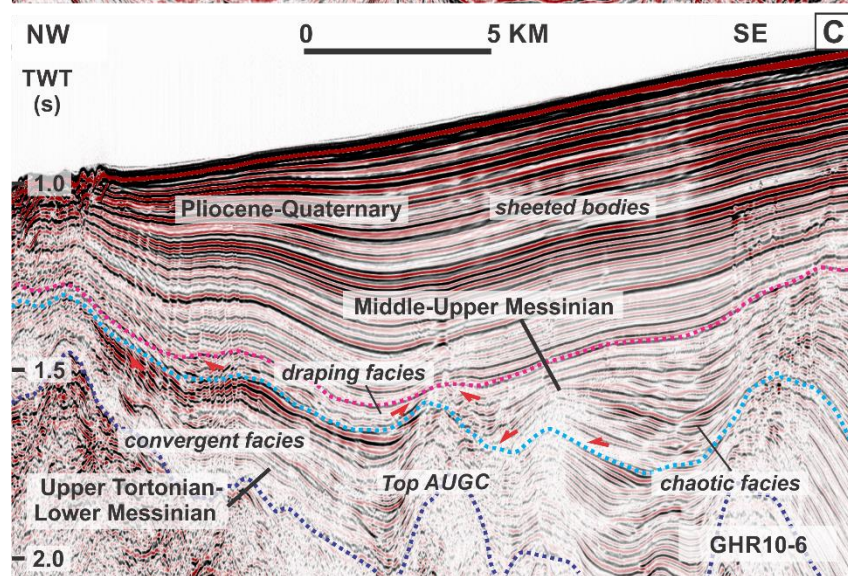
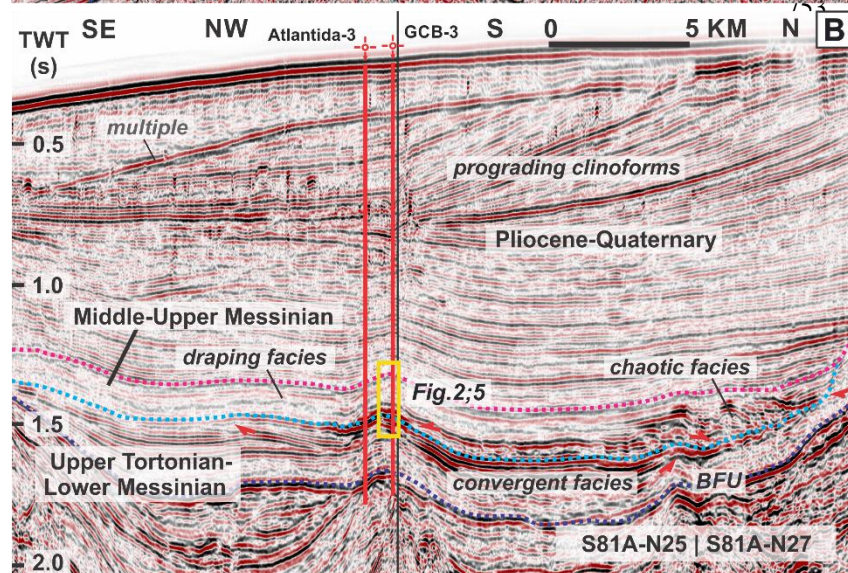
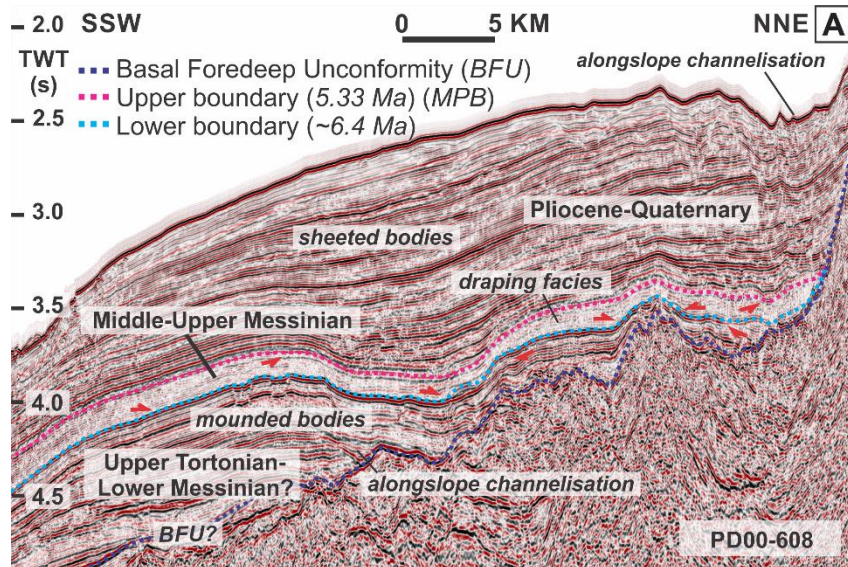
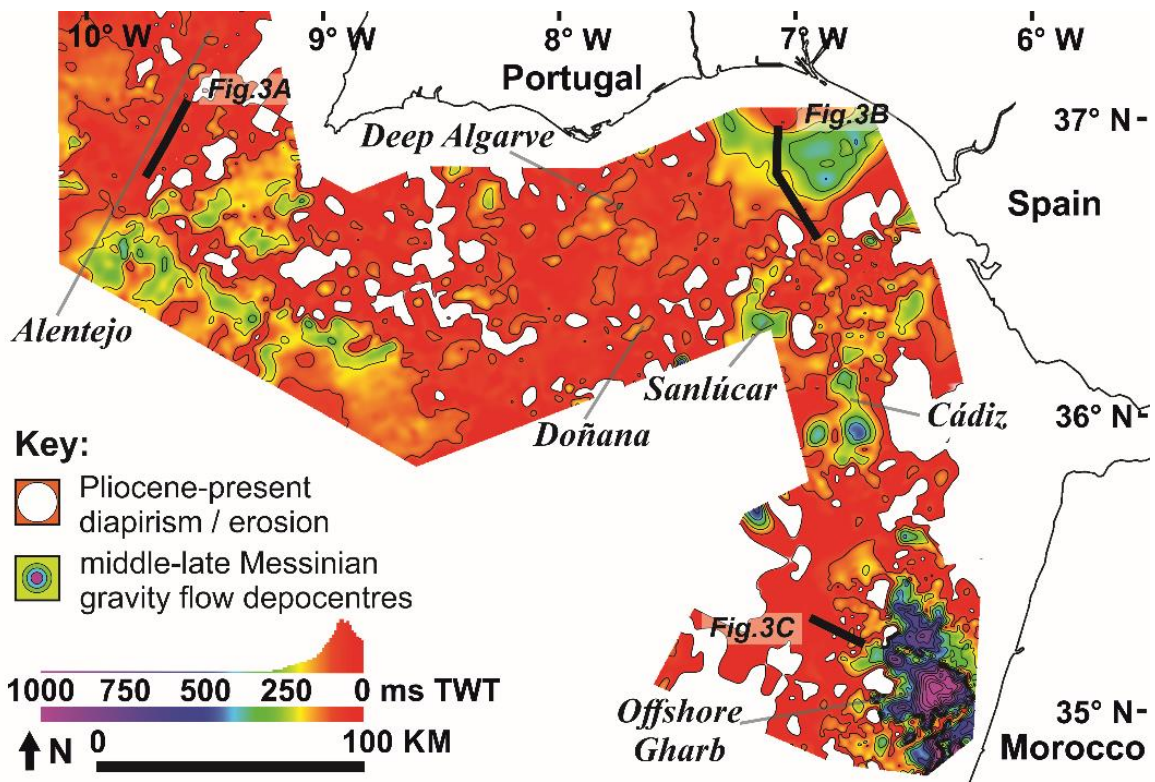


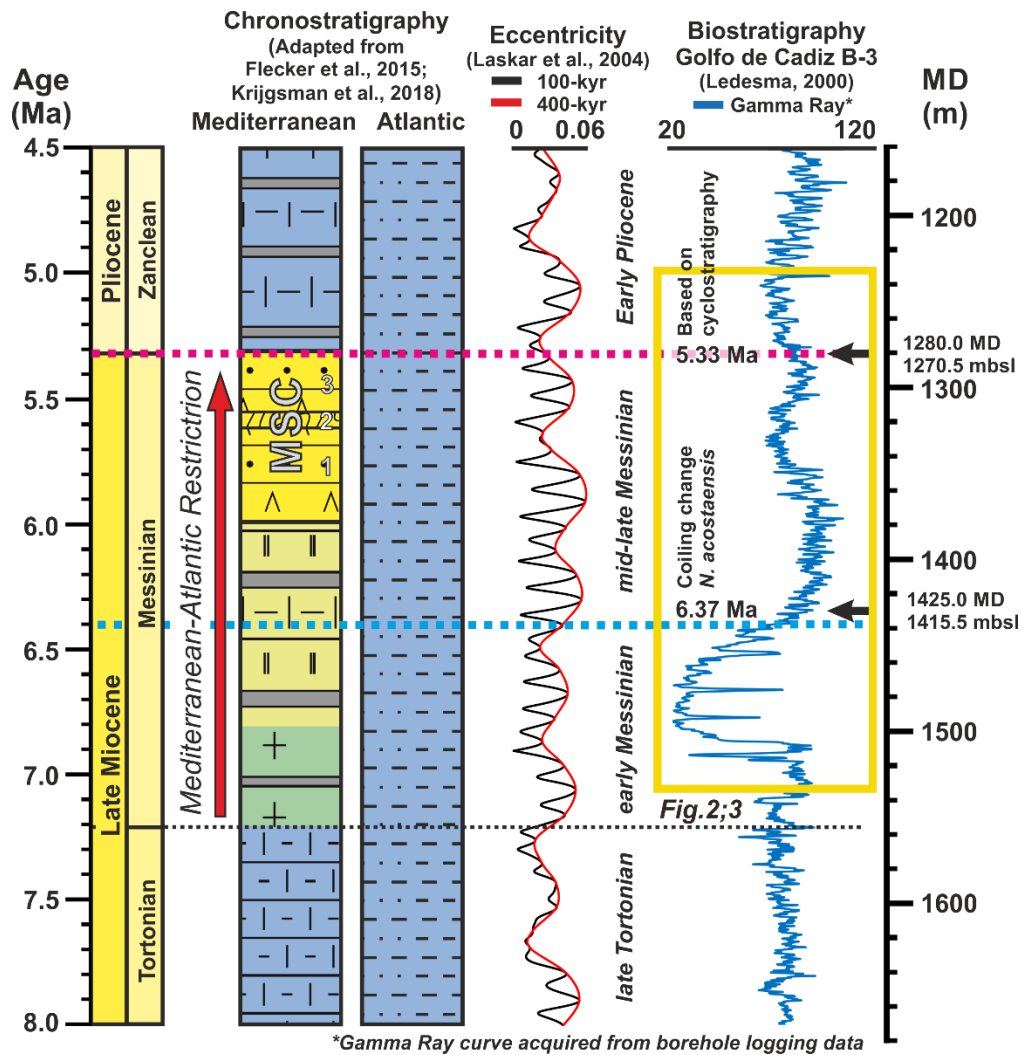
Figure 3. Seismic profiles indicating the distribution of the middle-upper Messinian unit across southern West Iberian margin (WIM): (a) PD00-608; (b) Southwest Iberian margin (SWIM): S81-N27 and S81-N25; and (c) Northwest Moroccan margin (NWMM): GHR10-6. Uninterpreted seismic profiles in Fig. S3 (supplementary material).



760

761 **Figure 4.** Time thickness (TWT) map of the middle-upper Messinian unit across Northwest Moroccan (NWMM),

762 Southwest Iberian (SWIM), and southern West Iberian (WIM) margins. (Contour interval: 100 ms TWT.)



763

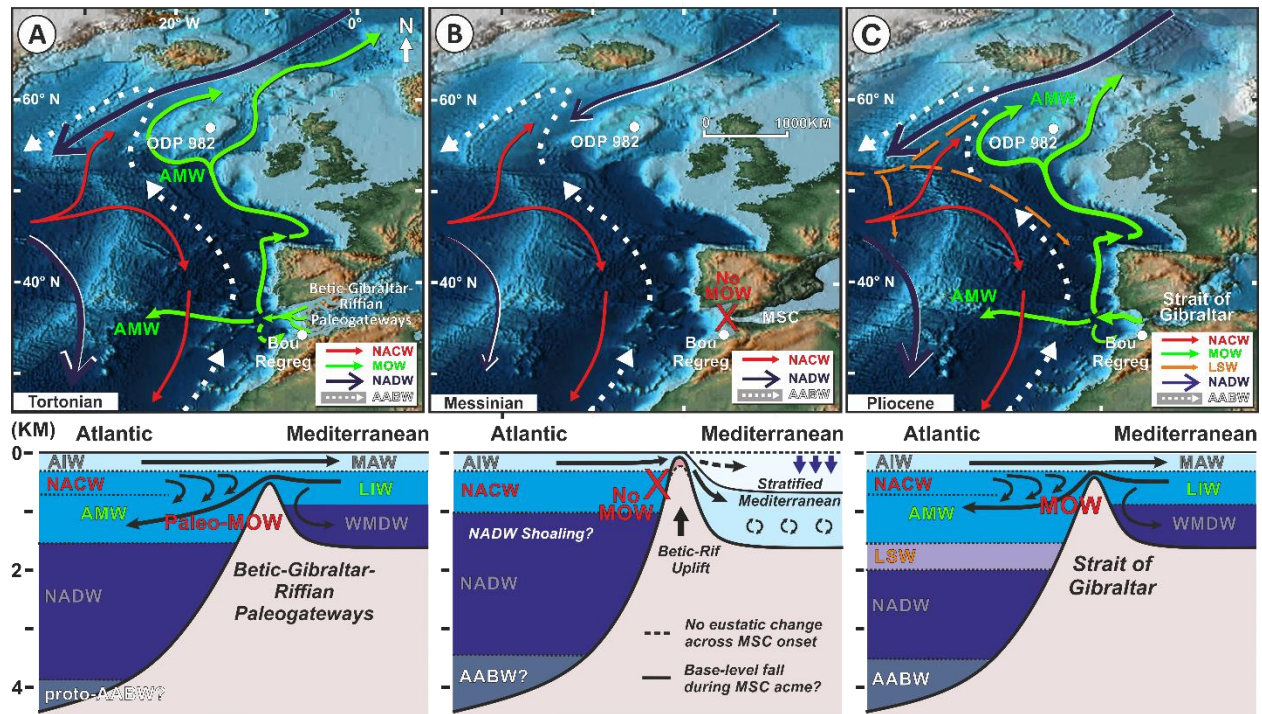
764

765

766

767

Figure 5. Chronology of middle-upper Messinian unit (right) and correlation with Mediterranean and Atlantic chronostratigraphy (Flecker et al., 2015; Krijgsman et al., 2018), 100 kyr and filtered 400 kyr eccentricity curves based on orbital solution La04 (Laskar et al., 2004), gamma ray logging in measured depth (MD) with biostratigraphy of well GCB-3 (Ledesma, 2000) in MD and meters below sea level (mbsl).



768

769 **Figure 6.** Scheme of the effect of Mediterranean-Atlantic restriction on the Atlantic Meridional Overturning
 770 Circulation (AMOC) during the (a) Tortonian, (b) Messinian, and (c) Pliocene. Paleogeographic reconstruction and
 771 Mediterranean-Atlantic gateway configuration adapted from Scotese (2014) and Krijgsman et al. (2018),
 772 respectively (NACW: North Atlantic Central Water; MOW: Mediterranean Outflow Water; LSW: Labrador Sea
 773 Water; NADW: North Atlantic Deep Water; AABW: Antarctic Bottom Water; AMW: Atlantic-Mediterranean
 774 Water.

